



NAVAL POSTGRADUATE SCHOOL

MONTEREY, CALIFORNIA

THESIS

**PERFORMANCE ANALYSIS OF A JTIDS/LINK-16 TYPE
WAVEFORM USING 32-ARY ORTHOGONAL SIGNALING
WITH 32 CHIP BASEBAND WAVEFORMS AND A
CONCATENATED CODE**

by

Theodoros Aivaliotis

December 2009

Thesis Advisor:
Second Reader:

R. Clark Robertson
Frank Kragh

Approved for public release; distribution unlimited

REPORT DOCUMENTATION PAGE			Form Approved OMB No. 0704-0188	
Public reporting burden for this collection of information is estimated to average 1 hour per response, including the time for reviewing instruction, searching existing data sources, gathering and maintaining the data needed, and completing and reviewing the collection of information. Send comments regarding this burden estimate or any other aspect of this collection of information, including suggestions for reducing this burden, to Washington headquarters Services, Directorate for Information Operations and Reports, 1215 Jefferson Davis Highway, Suite 1204, Arlington, VA 22202-4302, and to the Office of Management and Budget, Paperwork Reduction Project (0704-0188) Washington DC 20503.				
1. AGENCY USE ONLY (Leave blank)		2. REPORT DATE December 2009	3. REPORT TYPE AND DATES COVERED Master's Thesis	
4. TITLE AND SUBTITLE: Performance Analysis of a JTIDS/Link-16-type Waveform using 32-ary Orthogonal Signaling with 32 Chip Baseband Waveforms and a Concatenated Code			5. FUNDING NUMBERS	
6. AUTHOR(S) Theodoros Aivaliotis				
7. PERFORMING ORGANIZATION NAME(S) AND ADDRESS(ES) Naval Postgraduate School Monterey, CA 93943-5000			8. PERFORMING ORGANIZATION REPORT NUMBER	
9. SPONSORING / MONITORING AGENCY NAME(S) AND ADDRESS(ES) N/A			10. SPONSORING / MONITORING AGENCY REPORT NUMBER	
11. SUPPLEMENTARY NOTES The views expressed in this Thesis are those of the author and do not reflect the official policy or position of the Department of Defense or the U.S. Government.				
12a. DISTRIBUTION / AVAILABILITY STATEMENT Approved for public release; distribution is unlimited.			12b. DISTRIBUTION CODE A	
13. ABSTRACT (maximum 200 words) The Joint Tactical Information Distribution System (JTIDS) is a hybrid frequency-hopped, direct sequence spread spectrum system which uses cyclic code-shift keying (CCFK) for M -ary symbol modulation and minimum shift-keying (MSK) for chip modulation. In addition JTIDS uses a (31, 15) Reed Solomon (RS) code for channel coding. In this thesis an alternative waveform consistent with the original JTIDS waveform is analyzed. The system to be considered uses a concatenated code consisting of a (31, k) Reed Solomon inner code and a 4/5 convolutional outer code. The coded symbols are transmitted on the in-phase (I) and quadrature (Q) components of the carrier using 32-ary orthogonal signaling with 32 chip baseband waveforms such as Walsh functions. Performance with both coherent and noncoherent detection is analyzed. For noncoherent detection, only one five bit symbol is transmitted on the I and Q components of the carrier per symbol duration, so the data throughput for noncoherent detection is $\frac{1}{2}$ that of coherent detection. No diversity, consistent with JTIDS single-pulse structure, and a sequential diversity of two, consistent with JTIDS double-pulse structure, are both considered. For the double-pulse structure, performance is examined both for the case of linear soft diversity combining and also for soft diversity combining with perfect side information. Performance is examined both for AWGN only, as well as for AWGN and pulse-noise interference. Based on the results of this thesis, the proposed waveform is found to outperform the existing JTIDS/Link-16 waveform in all cases considered in this research. Indeed, the best performance for the alternative waveform is obtained when an (31, 25) RS inner code is used. When only AWGN is present, the proposed waveform with no diversity has a gain of 2.6 dB and 2.5 dB as compared to the existing JTIDS/Link-16 waveform for coherent and noncoherent demodulation, respectively, when $P_b = 10^{-5}$. Likewise, in an AWGN only environment with a diversity of two, the proposed waveform outperforms the existing JTIDS/Link-16 waveform by 3.15 dB and 2.3 dB for coherent and noncoherent detection, respectively. When PNI is also present, the proposed waveform performs significantly better than the existing JTIDS waveform in all cases considered. Finally, the use of a concatenated code consisting of a (31, 25) RS inner code and a 4/5 convolutional outer code results in a 33% improvement in throughput as compared to the existing JTIDS/Link-16 waveform.				
14. SUBJECT TERMS AWGN, CCSK, JTIDS, Link-16, MSK, probability of symbol error, Reed-Solomon codes, 32-ary Orthogonal signaling, Pulse-Noise interference (PNI), Diversity, Perfect-side information (PSI).			15. NUMBER OF PAGES 111	
			16. PRICE CODE	
17. SECURITY CLASSIFICATION OF REPORT Unclassified	18. SECURITY CLASSIFICATION OF THIS PAGE Unclassified	19. SECURITY CLASSIFICATION OF ABSTRACT Unclassified	20. LIMITATION OF ABSTRACT UU	

THIS PAGE INTENTIONALLY LEFT BLANK

Approved for public release; distribution is unlimited

**PERFORMANCE ANALYSIS OF A JTIDS/LINK-16 TYPE WAVEFORM USING
32-ARY ORTHOGONAL SIGNALING WITH 32 CHIP BASEBAND
WAVEFORMS AND A CONCATENATED CODE**

Theodoros Aivaliotis
Major, Hellenic Airforce
Bachelor, Hellenic Airforce Academy, 1993

Submitted in partial fulfillment of the
requirements for the degree of

MASTER OF SCIENCE IN ELECTRICAL ENGINEERING

from the

**NAVAL POSTGRADUATE SCHOOL
December 2009**

Author: Theodoros Aivaliotis

Approved by: R. Clark Robertson
Thesis Advisor

Frank Kragh
Second Reader

Jeffrey B. Knorr
Chair, Department of Electrical and Computer Engineering

THIS PAGE INTENTIONALLY LEFT BLANK

ABSTRACT

The Joint Tactical Information Distribution System (JTIDS) is a hybrid frequency-hopped, direct sequence spread spectrum system which uses cyclic code-shift keying (CCFK) for M -ary symbol modulation and minimum shift-keying (MSK) for chip modulation. In addition JTIDS uses a (31, 15) Reed Solomon (RS) code for channel coding. In this thesis an alternative waveform consistent with the original JTIDS waveform is analyzed. The system to be considered uses a concatenated code consisting of a (31, k) Reed Solomon inner code and a 4/5 convolutional outer code. The coded symbols are transmitted on the in-phase (I) and quadrature (Q) components of the carrier using 32-ary orthogonal signaling with 32 chip baseband waveforms such as Walsh functions. Performance with both coherent and noncoherent detection is analyzed. For noncoherent detection, only one five bit symbol is transmitted on the I and Q components of the carrier per symbol duration, so the data throughput for noncoherent detection is $\frac{1}{2}$ that of coherent detection. No diversity, consistent with JTIDS single-pulse structure, and a sequential diversity of two, consistent with JTIDS double-pulse structure, are both considered. For the double-pulse structure, performance is examined both for the case of linear soft diversity combining and also for soft diversity combining with perfect side information. Performance is examined both for AWGN only, as well as for AWGN and pulse-noise interference.

Based on the results of this thesis, the proposed waveform is found to outperform the existing JTIDS/Link-16 waveform in all cases considered in this research. Indeed, the best performance for the alternative waveform is obtained when an (31, 25) RS inner code is used. When only AWGN is present, the proposed waveform with no diversity has a gain of 2.6 dB and 2.5 dB as compared to the existing JTIDS/Link-16 waveform for coherent and noncoherent demodulation, respectively, when $P_b = 10^{-5}$. Likewise, in an AWGN only environment with a diversity of two, the proposed waveform outperforms the existing JTIDS/Link-16 waveform by 3.15 dB and 2.3 dB for coherent and noncoherent detection, respectively. When PNI is also present, the proposed waveform performs significantly better than the existing JTIDS waveform in all cases considered.

Finally, the use of a concatenated code consisting of a (31, 25) RS inner code and a 4/5 convolutional outer code results in a 33% improvement in throughput as compared to the existing JTIDS/Link-16 waveform.

TABLE OF CONTENTS

I.	INTRODUCTION.....	1
A.	OVERVIEW	1
B.	THESIS OBJECTIVE	1
C.	THESIS OUTLINE.....	2
II.	BACKGROUND	5
A.	<i>M</i>-ARY ORTHOGONAL MODULATION WITH BASEBAND WAVEFORMS.....	5
B.	PERFORMANCE OF <i>M</i>-ARY ORTHOGONAL SIGNALING IN AWGN.....	5
C.	PERFORMANCE OF <i>M</i>-ARY ORTHOGONAL SIGNALING IN AWGN WITH PULSE-NOISE INTERFERENCE.....	7
D.	CONCATENATED REED-SOLOMON AND CONVOLUTIONAL CODES.....	7
E.	PERFORMANCE WITH CONVOLUTIONAL AND REED- SOLOMON CODES.....	9
1.	Reed-Solomon Code.....	9
2.	Convolutional Codes.....	9
F.	PERFORMANCE WITH DIVERSITY	11
1.	Coherent Detection	12
2.	Noncoherent Detection	13
G.	PERFECT-SIDE INFORMATION	15
H.	CHAPTER SUMMARY.....	15
III.	PERFORMANCE ANALYSIS OF THE ORIGINAL JTIDS WAVEFORM	17
A.	BRIEF DESCRIPTION OF A JTIDS/LINK-16-TYPE SYSTEM.....	17
B.	COHERENT DEMODULATION.....	18
1.	AWGN Only Environment	18
2.	AWGN Plus PNI Environment.....	20
C.	NONCOHERENT DEMODULATION.....	21
1.	AWGN Only Environment	21
2.	AWGN Plus PNI Environment.....	22
D.	CHAPTER SUMMARY.....	23
IV.	PERFORMANCE ANALYSIS OF COHERENT AND NONCOHERENT ORTHOGONAL SIGNALING FOR A CONVOLUTIONAL CODE CONCATENATED WITH A RS CODE IN AWGN	25
A.	COHERENT DEMODULATION.....	25
B.	NONCOHERENT DEMODULATION.....	27
C.	COMPARISON BETWEEN COHERENT AND NONCOHERENT DEMODULATION FOR THE ALTERNATIVE WAVEFORM.....	29
D.	CHAPTER SUMMARY.....	30

V.	PERFORMANCE ANALYSIS OF COHERENT AND NONCOHERENT ORTHOGONAL SIGNALING WITH A CONVOLUTIONAL CODE CONCATENATED WITH A RS CODE IN AWGN AND PNI.....	31
A.	COHERENT DEMODULATION.....	31
B.	NONCOHERENT DEMODULATION.....	38
C.	COMPARISON BETWEEN COHERENT AND NONCOHERENT DEMODULATION FOR THE ALTERNATIVE WAVEFORM.....	45
D.	CHAPTER SUMMARY.....	47
VI.	PERFORMANCE ANALYSIS OF THE ALTERNATIVE JTIDS/LINK-16 WAVEFORM FOR BOTH COHERENT AND NONCOHERENT DEMODULATION IN AWGN ONLY WITH A DIVERSITY OF TWO.....	49
A.	COHERENT DEMODULATION.....	49
B.	NONCOHERENT DEMODULATION.....	51
C.	COMPARISON BETWEEN THE ALTERNATIVE WAVEFORM WITH A DIVERSITY OF TWO AND THE DOUBLE-PULSE STRUCTURE OF THE ORIGINAL JTIDS WAVEFORM IN AWGN..	53
D.	CHAPTER SUMMARY.....	54
VII.	PERFORMANCE ANALYSIS OF THE ALTERNATIVE JTIDS/LINK-16 WAVEFORM FOR BOTH COHERENT AND NONCOHERENT DEMODULATION IN AWGN AND PNI WITH A DIVERSITY OF TWO.....	55
A.	COHERENT DEMODULATION.....	55
B.	NONCOHERENT DEMODULATION.....	60
C.	COMPARISON BETWEEN COHERENT AND NONCOHERENT DEMODULATION FOR THE ALTERNATIVE WAVEFORM.....	66
D.	COMPARISON BETWEEN THE ALTERNATIVE WAVEFORM WITH A DIVERSITY OF TWO AND THE ORIGINAL JTIDS/LINK-16 DOUBLE-PULSE STRUCTURE WITH COHERENT DETECTION IN AWGN AND PNI.....	68
E.	CHAPTER SUMMARY.....	70
VIII.	PERFORMANCE ANALYSIS OF THE ALTERNATIVE JTIDS/LINK-16 WAVEFORM FOR BOTH COHERENT AND NONCOHERENT DEMODULATION IN AWGN AND PNI WITH A DIVERSITY OF TWO AND PSI.....	73
A.	COHERENT DEMODULATION.....	73
B.	NONCOHERENT DEMODULATION.....	78
C.	COMPARISON BETWEEN COHERENT AND NONCOHERENT DEMODULATION.....	83
D.	CHAPTER SUMMARY.....	84
IX.	CONCLUSIONS AND FUTURE WORK.....	85
	LIST OF REFERENCES.....	87
	INITIAL DISTRIBUTION LIST.....	89

LIST OF FIGURES

Figure 1.	Encoding and decoding configuration of the proposed system.	8
Figure 2.	A JTIDS/Link-16-type system model. From [4].....	17
Figure 3.	Performance of the JTIDS waveform in AWGN only environment and coherent demodulation.....	20
Figure 4.	Performance of the JTIDS waveform in an AWGN plus PNI environment and coherent demodulation for $E_b / N_0 = 10$ dB with $\rho = 1$, $\rho = 0.5$, and $\rho = 0.2$	21
Figure 5.	Performance of JTIDS with noncoherent demodulation in AWGN.....	22
Figure 6.	Performance of JTIDS with noncoherent demodulation for $E_b / N_0 = 10$ dB with $\rho = 1$, $\rho = 0.5$, and $\rho = 0.2$	23
Figure 7.	Encoding and decoding configuration of the proposed system.	25
Figure 8.	Performance of the alternative waveform with coherent demodulation in AWGN.....	27
Figure 9.	Performance of the alternative waveform with noncoherent demodulation in AWGN.....	28
Figure 10.	Comparison of the performance of the coherent and noncoherent demodulation for the proposed waveform in AWGN.....	29
Figure 11.	Performance of the proposed waveform in both AWGN and PNI with coherent demodulation for $\rho = 1$, $\rho = 0.5$, $\rho = 0.2$, $\rho = 0.1$ and $\rho = 0.05$ when $E_b / N_0 = 4.7$ dB.....	33
Figure 12.	Performance of the original JTIDS/Link-16 waveform in both AWGN and PNI with coherent demodulation for $\rho = 1$, $\rho = 0.5$, $\rho = 0.2$ and $\rho = 0.1$ when $E_b / N_0 = 4.7$ dB.....	34
Figure 13.	Performance of the alternative waveform in both AWGN and PNI with coherent demodulation for $\rho = 1$, $\rho = 0.5$, $\rho = 0.2$, $\rho = 0.1$, and $\rho = 0.05$ when $E_b / N_0 = 8.4$ dB.....	35
Figure 14.	Performance of the original JTIDS/Link-16 waveform in both AWGN and PNI with coherent demodulation for $\rho = 1$, $\rho = 0.5$, $\rho = 0.2$, $\rho = 0.1$, and $\rho = 0.05$ when $E_b / N_0 = 8.4$ dB.	36
Figure 15.	Performance of the alternative waveform in both AWGN and PNI with noncoherent demodulation for $\rho = 1$, $\rho = 0.5$, $\rho = 0.2$, $\rho = 0.1$, and $\rho = 0.05$ when $E_b / N_0 = 6$ dB.....	40
Figure 16.	Performance of the original JTIDS/Link-16 waveform in both AWGN and PNI with noncoherent demodulation for $\rho = 1$, $\rho = 0.5$, $\rho = 0.2$ and $\rho = 0.1$ when $E_b / N_0 = 6$ dB.....	41
Figure 17.	Performance of the alternative waveform in both AWGN and PNI with noncoherent demodulation for $\rho = 1$, $\rho = 0.5$, $\rho = 0.2$, $\rho = 0.1$, and $\rho = 0.05$ when $E_b / N_0 = 8.4$ dB.	42

Figure 18.	Performance of the original JTIDS/Link-16 waveform in both AWGN and PNI with noncoherent demodulation for $\rho = 1$, $\rho = 0.5$, $\rho = 0.2$, $\rho = 0.1$, and $\rho = 0.05$ when $E_b / N_0 = 8.4$ dB.	43
Figure 19.	Comparison of the performance of the alternative waveform with both AWGN and PNI for coherent and noncoherent demodulation when $E_b / N_0 = 8.4$ dB for $\rho = 1$, and $\rho = 0.1$	46
Figure 20.	Performance of the alternative waveform with coherent demodulation for both no diversity and a diversity of two in AWGN.	50
Figure 21.	Performance of the alternative waveform with noncoherent demodulation for both no diversity and diversity of two in AWGN.	52
Figure 22.	Performance of both the alternative waveform with a diversity of two and the existing JTIDS/Link-16 double-pulse structure for coherent and noncoherent detection in AWGN.	53
Figure 23.	Performance of the alternative waveform in both AWGN and PNI for coherent demodulation with a diversity of two for $\rho = 1$, $\rho = 0.5$, $\rho = 0.2$, $\rho = 0.1$, $\rho = 0.05$, and $\rho = 0.03$ when $E_b / N_0 = 4.7$ dB.	57
Figure 24.	Performance of the alternative waveform in both AWGN and PNI environment with coherent demodulation with a diversity of two for $\rho = 1$, $\rho = 0.5$, $\rho = 0.2$, $\rho = 0.1$, $\rho = 0.05$, and $\rho = 0.02$ when $E_b / N_0 = 1.37$ dB.	59
Figure 25.	Performance of the alternative waveform in both AWGN and PNI with noncoherent demodulation with a diversity of two for $\rho = 1$, $\rho = 0.5$, $\rho = 0.2$, and $\rho = 0.1$ when $E_b / N_0 = 6$ dB.	63
Figure 26.	Performance of the alternative waveform in both AWGN and PNI with noncoherent demodulation and a diversity of two for $\rho = 1$, $\rho = 0.5$, $\rho = 0.2$, $\rho = 0.1$, $\rho = 0.05$, and $\rho = 0.02$ when $E_b / N_0 = 3.11$ dB.	65
Figure 27.	Comparison of the performance of the alternative waveform with a diversity of two for coherent and noncoherent detection in AWGN and PNI for $\rho = 1$ and $\rho = 0.05$ when $E_b / N_0 = 3.11$ dB.	67
Figure 28.	Performance of the alternative waveform with a diversity of two and the original JTIDS/Link-16 double-pulse structure with coherent demodulation in AWGN and PNI when $E_b / N_0 = 7.78$ dB for $\rho = 1$ and $\rho = 0.1$	69
Figure 29.	Performance of the alternative waveform with a diversity of two for coherent detection in AWGN and PNI with PSI when $E_b / N_0 = 4.7$ dB for $\rho = 1$, $\rho = 0.5$, and $\rho = 0.2$	75
Figure 30.	Performance of the alternative waveform with a diversity of two for coherent detection in AWGN and PNI with PSI when $E_b / N_0 = 1.37$ dB for $\rho = 1$, $\rho = 0.5$, $\rho = 0.2$, $\rho = 0.1$, and $\rho = 0.05$	77
Figure 31.	Performance for noncoherent detection in AWGN and PNI with PSI when $E_b / N_0 = 6$ dB for $\rho = 1$, $\rho = 0.5$, and $\rho = 0.2$	79

Figure 32.	Performance of the alternative waveform with a diversity of two for noncoherent detection in AWGN and PNI with PSI when $E_b / N_0 = 3.11$ dB for $\rho = 1, \rho = 0.5, \rho = 0.2, \rho = 0.1,$ and $\rho = 0.05$81
Figure 33.	Comparison of the performance of the alternative waveform with a diversity of two and PSI between coherent and noncoherent detection in AWGN and PNI for $\rho = 1$ and $\rho = 0.5$ when $E_b / N_0 = 6$ dB.83

THIS PAGE INTENTIONALLY LEFT BLANK

LIST OF TABLES

Table 1.	Conditional probabilities of symbol error for the 32-chip CCSK sequence chosen for JTIDS. From [4].....	18
Table 2.	Comparison of the performance of the alternative waveform for coherent and noncoherent demodulation when $P_b = 10^{-5}$ in AWGN.....	30
Table 3.	Comparison of the performance of the original JTIDS/Link-16 and the alternative waveforms for different values of ρ for coherent demodulation when $E_b / N_0 = 4.7$ dB.....	37
Table 4.	Comparison of the performance of the original JTIDS/Link-16 and the alternative waveforms for different values of ρ for coherent demodulation when $E_b / N_0 = 8.4$ dB.....	38
Table 5.	Comparison of the performance of the original JTIDS/Link-16 and the alternative waveforms for different values of ρ for noncoherent demodulation when $E_b / N_0 = 6$	44
Table 6.	Comparison of the performance of the original JTIDS/Link-16 and the alternative waveforms for different values of ρ for noncoherent demodulation when $E_b / N_0 = 8.4$ dB.....	45
Table 7.	Comparison between coherent and noncoherent demodulation of the alternative waveform in AWGN and PNI when $P_b = 10^{-5}$ and $E_b / N_0 = 8.4$ dB for $\rho = 1$, and $\rho = 0.1$	47
Table 8.	Comparison of the performance of the alternative waveform for coherent demodulation in AWGN when $P_b = 10^{-5}$	50
Table 9.	Comparison of the performance of the alternative waveform for noncoherent demodulation in AWGN when $P_b = 10^{-5}$	52
Table 10.	Comparison between the alternative waveform with a diversity of two and the double-pulse structure of the existing JTIDS in AWGN when $P_b = 10^{-5}$	54
Table 11.	Comparison of the performance of the alternative waveform with coherent demodulation in both AWGN and PNI for no diversity and a diversity of two when $P_b = 10^{-5}$	58
Table 12.	Required E_b / N_1 for $P_b = 10^{-5}$ when $E_b / N_0 = 1.37$ dB for the alternative waveform in both AWGN and PNI with coherent detection and a diversity of two.....	60
Table 13.	Comparison of the performance of the alternative waveform with noncoherent demodulation in both AWGN and PNI for no diversity and a diversity of two for $P_b = 10^{-5}$ [From author].....	64
Table 14.	Required E_b / N_1 for $P_b = 10^{-5}$ when $E_b / N_0 = 3.11$ dB for the alternative waveform in both AWGN and PNI with noncoherent detection and a diversity of two.....	66

Table 15.	Comparison between coherent and noncoherent demodulation for the alternative waveform in an AWGN plus PNI environment with a diversity of two when $P_b = 10^{-5}$ and $E_b / N_0 = 3.11$ dB for $\rho = 1$ and $\rho = 0.05$	68
Table 16.	Comparison between the alternative waveform with a diversity of two and the double-pulse structure of the existing JTIDS in AWGN and PNI when $E_b / N_0 = 7.78$ dB and $P_b = 10^{-5}$	70
Table 17.	Comparison between the diversity of two structure of the alternative waveform in AWGN and PNI with coherent demodulation and no-side information and the same structure with PSI when $E_b / N_0 = 4.7$ dB.	76
Table 18.	Comparison between the diversity of two structure of the alternative waveform in AWGN and PNI with coherent demodulation and no-side information and the same structure with PSI when $E_b / N_0 = 1.37$ dB.	78
Table 19.	Comparison between the diversity of two structure of the alternative waveform in AWGN and PNI with noncoherent demodulation and no-side information and the same structure with PSI when $E_b / N_0 = 6$ dB.	80
Table 20.	Comparison between the diversity of two structure of the alternative waveform in AWGN and PNI with noncoherent demodulation and no-side information and the same structure with PSI when $E_b / N_0 = 3.11$ dB.	82
Table 21.	Comparison between coherent and noncoherent demodulation for the alternative waveform in AWGN and PNI with a diversity of two and PSI when $P_b = 10^{-5}$ and $E_b / N_0 = 6$ dB for $\rho = 1$ and $\rho = 0.5$	84

EXECUTIVE SUMMARY

The Tactical Data Link (TDL) is a solution to the reliability problems of primitive communication systems. TDLs are the cornerstone of the Network Centric Warfare (NCW) concept, not only because they provide full situational awareness to headquarter units, but also because they enable secure and reliable communication as well. The most widely spread TDL today is the Joint Tactical Information Distribution System (JTIDS) which is commonly referred to as Link-16. JTIDS/Link-16 was born out of the difficulties the United States found itself in during the Vietnam War when trying to coordinate the effort of many different elements of its armed forces. Battlefield cooperation among all branches of the U.S. armed forces was required. Earlier TDLs, Link-4, Link-11 and Link-14, were each restricted in function and implementation and often available only to specific elements of a specific force.

JTIDS/Link-16 provides tremendous flexibility and has proven to be very useful operationally. It is usually regarded as a jam resistant data link. JTIDS is a hybrid frequency-hopped, direct sequence spread spectrum system which uses cyclic code-shift keying (CCFK) for M -ary symbol modulation and minimum-shift keying (MSK) for chip modulation. In addition JTIDS uses a (31, 15) Reed Solomon (RS) code for channel coding. In this thesis an alternative waveform consistent with the original JTIDS waveform is analyzed. The system to be considered uses a concatenated code consisting of a (31, k) Reed Solomon inner code and a $4/5$ convolutional outer code. The coded symbols are transmitted on the in-phase (I) and quadrature (Q) components of the carrier using 32-ary orthogonal signaling with 32 chip baseband waveforms such as Walsh functions. Performance for both coherent and noncoherent detection is analyzed. For noncoherent detection, only one five bit symbol is transmitted on the I and Q components of the carrier per symbol duration, so the data throughput for noncoherent detection is $\frac{1}{2}$ that of coherent detection. No diversity, consistent with the JTIDS single-pulse structure and a sequential diversity of two, consistent with the JTIDS double-pulse structure, are both considered. For the double-pulse structure, performance is examined both for the

case of linear soft diversity combining and also for soft diversity combining with perfect side information. Performance is examined both for AWGN only as well as for both AWGN and pulse-noise interference.

Based on the results of this thesis, the proposed waveform is found to outperform the existing JTIDS/Link-16 waveform in all cases considered in this research. Indeed, the best performance for the alternative waveform is obtained when an (31, 25) RS inner code is used. When only AWGN is present, the proposed waveform with no diversity has a gain of 2.6 dB and 2.5 dB compared to the existing JTIDS/Link-16 waveform for coherent and noncoherent demodulation, respectively, when $P_b = 10^{-5}$. Likewise, in an AWGN only environment with a diversity of two, the proposed waveform outperforms the existing JTIDS/Link-16 waveform by 3.15 dB and 2.3 dB for coherent and noncoherent detection, respectively. When PNI is also present, the proposed waveform performs significantly better than the existing JTIDS in all cases considered. Finally, the use of a concatenated code consisting of a (31, 25) RS inner code and 4/5 convolutional code results in a 33% improvement in throughput, as compared to the existing JTIDS/Link-16 waveform.

LIST OF ACRONYMS AND ABBREVIATIONS

AWGN	Additive White Gaussian Noise
BCH	Bose Chaudhuri Hocquenghem
CCSK	Cyclic Code Shift Keying
DS	Direct Sequence
EED	Errors and Erasures Decoding
FH	Frequency Hopped
ISR	Imagery Support Requirement
JTIDS	Joint Tactical Information Distribution System
MFSK	M-ary Frequency Shift Keying
MSK	Minimum Shift Keying
NATO	North Atlantic Treaty Organization
NCW	Network Centric Warfare
PDF	Probability Density Function
PNI	Pulse Noise Interference
PSD	Power Spectral Density
PSI	Perfect Side Information
RS	Reed-Solomon
STDP	Standard Double Pulse
TDL	Tactical Data Link

THIS PAGE INTENTIONALLY LEFT BLANK

ACKNOWLEDGMENTS

As you set out for Ithaca hope your road is a long one, full of adventure, full of discovery. Laistrygonians, Cyclops, angry Poseidon - don't be afraid of them: you' ll never find things like that on your way as long as you keep your thoughts raised high, as long as a rare excitement stirs your spirit and your body. Laistrygonians, Cyclops, wild Poseidon—you won't encounter them unless you bring them along inside your soul, unless your soul sets them up in front of you...

From the poem "Ithaca" by
Konstantinos Kavafis (1911)

I would like to thank Professor Robertson for his valuable help and guidance, and all the other professors and teachers who made my journey into knowledge a long worthwhile experience.

At most I would like to thank *Ηρώ* for being an 'impulse' of poetry in my life for twenty years.

THIS PAGE INTENTIONALLY LEFT BLANK

I. INTRODUCTION

A. OVERVIEW

The Tactical Data Link (TDL) is a solution to the reliability and security problems of basic communication systems. In telecommunications, a data link is the means of connecting one location to another for the purpose of transmitting and receiving digital information. It can also refer to a set of electronic assemblies, consisting of a transmitter and a receiver and the interconnecting data telecommunication circuit. These are governed by a link protocol enabling digital data to be transferred from a data source to a data sink [1]. Tactical Data Links are the corner stone of the Network Centric Warfare (NCW) concept, not only because they provide full situational awareness to headquarter units but also because they enable secure and reliable communication. The most widely spread Tactical Data Link currently is the Joint Tactical Information Distribution System (JTIDS), which is the communication component of Link-16.

JTIDS/Link-16 is secure and provides a measure of resistance to jamming. JTIDS/Link-16 is a hybrid direct sequence, frequency hopped spread spectrum system that employs time-division multiple access as well. JTIDS/Link-16 is not without its limitations, the most important of which is its limited data throughput. This constrains its usage to situational awareness functions, command and control, low data rate ISR imagery functions, and other functions such as weapon guidance [2].

B. THESIS OBJECTIVE

Because of its reliability and the other advantages mentioned previously, JTIDS/Link-16 currently is the most common NATO TDL. However, the need for a TDL with greater throughput drives the research for enhanced versions compatible with the original JTIDS which will increase throughput without requiring additional signal power.

Some alternative waveforms consistent with the existing JTIDS waveform but with better performance have been considered. In [3], the cyclical code-shift keying (CCSK) modulation scheme used by the original JTIDS/Link-16 was replaced with 32-ary orthogonal signaling having 32 chip baseband waveforms. In [4], two modified

JTIDS/Link-16 compatible systems are proposed and evaluated. The first system uses errors-and-erasures decoding (EED) in place of errors-only RS decoding, whereas the second system employs a new 32-chip CCSK sequence instead of the 32-chip CCSK sequence chosen for JTIDS/Link-16. In [5] a 32-ary CCSK system that uses a concatenated code consisting of a rate $r = 4/5$ convolutional code as an outer code and a $(31, k)$ RS code as an inner code is considered.

In this thesis, an alternative waveform consistent with the original JTIDS waveform is analyzed. The system to be considered uses a concatenated code consisting of a $(31, k)$ Reed Solomon (RS) inner code and a $4/5$ convolutional outer code. The coded symbols are transmitted on the in-phase (I) and quadrature (Q) components of the carrier using 32-ary orthogonal signaling with 32 chip base band waveforms such as Walsh functions. Performance with both coherent and non-coherent detection is analyzed. For non-coherent detection, only one five bit symbol is transmitted on the I and Q components of the carrier per symbol duration, so the data throughput for non-coherent detection is $1/2$ that of coherent detection. No diversity, consistent with the JTIDS single-pulse structure, and a sequential diversity of two, consistent with the JTIDS double-pulse structure, are both considered. For the double-pulse structure, performance is examined both for the case of linear-soft diversity combining and also for soft diversity combining with perfect side information. Performance will be examined both for additive white Gaussian noise (AWGN) only as well as for AWGN plus pulse-noise interference (PNI).

C. THESIS OUTLINE

This thesis is organized into nine chapters. Chapter I is the introduction. Chapter II is the theoretical background which the author considers necessary to understand this research. Chapter III deals with the performance analysis of the original JTIDS waveform, which is the reference point for the performance of the alternative waveform. In Chapter IV, the performance analysis of the alternative waveform in an AWGN environment for both coherent and noncoherent demodulation is discussed. In addition the number of uncoded symbols k in the $(31, k)$ RS code that yield the minimum probability of bit error at the output of the receiver is determined. In Chapter V, the performance analysis of the alternative waveform in an AWGN plus PNI environment for

both coherent and noncoherent demodulation is analyzed. In Chapter VI, the performance analysis of the proposed waveform in an AWGN only environment with a diversity of two for both coherent and noncoherent demodulation is considered. In Chapter VII, the performance analysis of the proposed waveform in an AWGN plus PNI environment with a diversity of two for both coherent and noncoherent demodulation is discussed. In Chapter VIII, the performance analysis of the alternative waveform with a diversity of two and perfect side information (PSI) is analyzed. Finally, the conclusions to this thesis are presented in Chapter IX.

THIS PAGE INTENTIONALLY LEFT BLANK

II. BACKGROUND

In this chapter, some of the key concepts needed for the analysis of the proposed alternative JTIDS waveform are discussed. Concepts and equations that have been extensively described in the existing literature will be presented for the convenience of the reader. On the other hand, concepts and equations that are more specialized are derived more thoroughly.

A. *M*-ARY ORTHOGONAL MODULATION WITH BASEBAND WAVEFORMS

The alternative waveform analyzed in this thesis uses *M*-ary orthogonal modulation with baseband waveforms. More specifically, 32 orthogonal baseband waveforms are used to modulate the transmitted signal. In orthogonal signaling the data symbols can be modulated on both the I and the Q channel simultaneously, improving significantly the overall throughput when coherent detection is used.

The probability of symbol error and the probability of bit error of a system that utilizes *M*-ary signaling with orthogonal baseband waveforms are identical to those for orthogonal *M*-ary frequency-shift keying (*MFSK*), as are the union bounds on the probabilities of symbol and bit error [6].

One advantage of using *M*-ary orthogonal modulation with orthogonal baseband waveforms instead of orthogonal frequencies is that the former naturally combines with direct sequence spread spectrum, whereas *MFSK* does not. Thus, an *M*-ary orthogonal baseband waveform is compatible with the original JTIDS waveform. Another advantage of this modulation technique over orthogonal *MFSK* is that it requires only one local oscillator at the receiver rather than *M* and, hence, the complexity of the overall system is reduced [6].

B. PERFORMANCE OF *M*-ARY ORTHOGONAL SIGNALING IN AWGN

The probability of channel symbol error for both coherent and noncoherent detection can be expressed in two different ways depending on the derivation method.

For the coherent case in AWGN with two-sided noise power spectral density $N_o / 2$, the probability of symbol error can be expressed either as a union bound [6]

$$P_s \leq (M - 1)Q\left(\sqrt{\frac{rE_s}{N_o}}\right) \quad (2.1)$$

or as an exact value [6]

$$P_s = \frac{1}{\sqrt{2\pi}} \int_{-\infty}^{\infty} e^{\left(\frac{-u^2}{2}\right)} \left\{ 1 - \left[1 - Q\left(u + \sqrt{\frac{2rE_s}{N_o}}\right) \right]^{M-1} \right\} du, \quad (2.2)$$

where E_s is the average energy per channel symbol, $E_s = A_c^2 T_s$, T_s is the symbol duration, r is the code rate, and A_c^2 is the received signal power.

Both of the preceding formulas yield accurate results for the AWGN case; however, when the channel is affected by both AWGN and PNI, equation (2.2) must be used for greater accuracy.

Analogously, there are two options as well when noncoherent detection is used. Again, the union bound can be used in an AWGN only environment without any adverse effects on the accuracy of the result, while the exact result must be used for an AWGN plus PNI environment. The union bound and the exact results for the noncoherent case are [6]

$$P_s \leq \frac{M - 1}{2} \exp\left(\frac{-rE_s}{2N_o}\right) \quad (2.3)$$

and

$$P_s = \sum_{n=1}^{M-1} \frac{(-1)^{n+1}}{n+1} \binom{M-1}{n} \exp\left[\frac{-nrE_s}{(n+1)N_o}\right], \quad (2.4)$$

respectively.

C. PERFORMANCE OF *M*-ARY ORTHOGONAL SIGNALING IN AWGN WITH PULSE-NOISE INTERFERENCE

When a channel is affected by AWGN the noise signal that arrives at the receiver is assumed to be uniformly spread across the spectrum and time independent, but those assumptions may not be valid if PNI is present. In this thesis, the AWGN and PNI are assumed to be statistically independent, and the PNI is modeled as Gaussian noise. When AWGN and PNI are both present the total noise power at the receiver integrator outputs is given by

$$\sigma_x^2 = \sigma_{WG}^2 + \sigma_I^2 \quad (2.5)$$

where $\sigma_{WG}^2 = N_0/T_s$ and $\sigma_I^2 = N_I / \rho T_s$, ρ is the fraction of time that the PNI is on, and N_I is the PNI one-sided power spectral density [3].

By assuming that each symbol is short compared to the pulse-noise interference on-time, we can infer that even if some symbols are only partially affected by the PNI their number (and thus their contribution to the overall probability of error) is negligible compared to those which are either free of interference or entirely affected. Consequently, when PNI is present the average probability of channel symbol error for hard decision demodulation is

$$P_s = \rho P_s[E_s / (N_0 + N_I / \rho)] + (1 - \rho) P_s(E_s / N_0) \quad (2.6)$$

where $P_s[E_s / (N_0 + N_I / \rho)]$ and $P_s(E_s / N_0)$ are the probabilities of symbol error in the presence or in the absence of PNI, respectively.

D. CONCATENATED REED-SOLOMON AND CONVOLUTIONAL CODES

A concatenated code is one that uses two levels of coding, an inner code and an outer code, to achieve improved error performance. The inner code, the one that interfaces with the modulator/demodulator and channel, is usually configured to correct most of the channel errors. The outer code, usually a higher-rate code, then reduces the probability of error to a specified level. The primary reason for using a concatenated code is to achieve a low error rate with an overall implementation complexity which is less than that which would be required by a single coding operation [7].

In this thesis a convolutional code with code rate $4/5$ is used as the outer code while a Reed-Solomon code with a code rate $k/31$ (an optimum k is determined) is used as the inner code. Figure 1 illustrates the order of encoding and decoding. This configuration is preferred since it can be implemented with fewer bit-to-symbol and symbol-to-bit converters. In this implementation, only one bit-to-symbol converter is used in the transmitter and one symbol-to-bit converter in the receiver. With the proposed configuration, blocks of four data bits are encoded into five-bit blocks which then are encoded into five-bit symbols. At the inner encoder, k symbols are encoded into 31 channel symbols which then are modulated by a 32-ary orthogonal modulator. The overall code-rate is $4k / (5 \times 31)$ while the code-rate of JTIDS is $15 / 31 = 0.484$. Hence, in addition to the improvement in the bit error performance a significant throughput increase is obtained when $k > 19$. Taking the ratio of the code rate of the proposed system to that of the original JTIDS, we get the change in throughput effectuated by the proposed system:

$$T = \frac{4k}{75}. \quad (2.7)$$

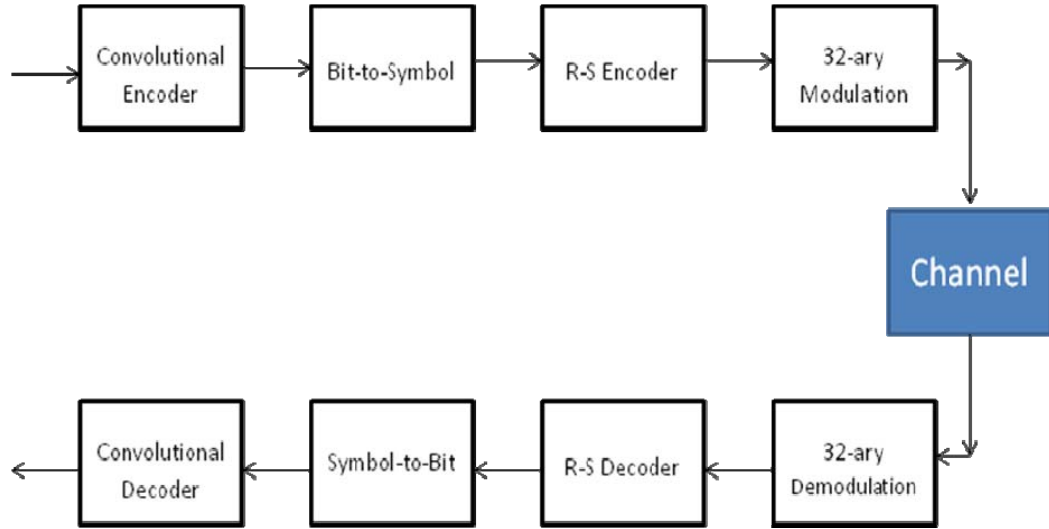


Figure 1. Encoding and decoding configuration of the proposed system.

E. PERFORMANCE WITH CONVOLUTIONAL AND REED-SOLOMON CODES

The probability of information bit error is expected to be improved by the concatenated code. In order to derive the probability of bit error at the output of the receiver, we need to determine the effect of both the Reed-Solomon (inner) code and the convolutional (outer) code on the probability of bit error.

1. Reed-Solomon Code

Reed-Solomon codes are nonbinary BCH (Bose–Chaudhuri–Hocquenghem) codes. An (n, k) RS encoder takes k information symbols and generates n coded symbols [8]. For nonbinary codes, the distance between two code words is defined (analogous to Hamming distance) as the number of symbols in which the codewords differ. Reed-Solomon codes achieve the largest possible code minimum distance for any linear code with the same encoder input and output block lengths [7]. The last property as well as the fact that RS can be designed with different amounts of redundancy makes them the most commonly used nonbinary block codes for random error correction.

The Reed-Solomon decoded symbol error probability, in terms of the channel symbol error probability, is [8]

$$P_s = \frac{1}{n} \sum_{i=t+1}^n i \binom{n}{i} P_s^i (1 - P_s)^{n-i} \quad (2.8)$$

where P_s is the channel symbol error probability, t is the symbol error correcting capability of the RS code, $n = 2^m - 1$, and m is the number of bits per encoded symbol.

2. Convolutional Codes

The main difference in convolutional codes as compared to block codes, such as the Reed-Solomon code mentioned previously, is the fact that with block codes, each codeword n -tuple is uniquely determined by the input message k -tuple, whereas in the former this is not the case. In a convolutional code the ratio k/n has the same significance (information per coded bit) that it has for block codes; however, n does not define a block or codeword length as it does for block codes. An n -tuple emitted by the convolutional

encoding procedure is not only a function of an input k -tuple but is also a function of the previous $K-1$ input k -tuples, where K is a parameter known as the constraint length [7].

Since the convolutional code output does not necessarily have a fixed length, we derive its performance from the probability of sequences that merge with the all-zero sequence (provided that the all-zero sequence is transmitted) for the first time at a given node in the trellis. In particular, we define the first-event error probability as the probability that another path that merges with the all-zero path at node B has a metric that exceeds the metric of the all-zero path for the first time. Of course, in the transmission of signals that are convolutionally encoded, other types of errors can occur; but it can be shown that bounding the error probability of the convolutional code by the sum of first-event error probabilities provides an upper bound that in most cases is a tight upper bound on the error probability. For hard decision decoding, we can employ exact expressions for the pair-wise error probability to obtain tighter bounds on the error probability. The probability of selecting a path of weight d , when d is odd, over the all-zero path is the probability that the number of errors is greater than or equal to $(d+1)/2$ [9]. Therefore, the pair-wise error probability is given by

$$P_2(d) = \sum_{k=(d+1)/2}^d \binom{d}{k} p^k (1-p)^{d-k} \quad (2.9)$$

If d is even, the incorrect path is selected when the number of errors exceeds $0.5d$. If the number of errors equals $0.5d$, there is a tie between the metrics of the two paths which is resolved by randomly selecting one of the paths; thus, an error occurs one-half the time. Consequently, the pair-wise error probability in this case is given by [9]

$$P_2(d) = \frac{1}{2} \binom{d}{d/2} p^{d/2} (1-p)^{d/2} + \sum_{k=d/2+1}^d \binom{d}{k} p^k (1-p)^{d-k} \quad (2.10)$$

The overall bit error probability is bounded by [9]

$$P_b \leq \frac{1}{k} \sum_{d=d_{free}}^{\infty} \beta_d P_2(d) \quad (2.11)$$

where k is the number of information bits per level (number of bits encoded per clock cycle), and β_d is the sum of all possible bit errors that can occur on all paths a distance d

from the all-zero code sequence. In this thesis we consider $d=5$ which corresponds to the free distance for an encoder with eight memory elements and code rate $4/5$. The corresponding generator polynomials (in octal) are 561,753,561,753,561 and $\beta_5 = 5$ [10].

F. PERFORMANCE WITH DIVERSITY

Diversity is the procedure that consists of transmitting and/or receiving the same symbol multiple times in order to provide redundancy at the receiver. The basic idea of diversity is that some of the received redundant symbols will be more reliable than others, and the demodulation decision will be made using the more reliable symbols [6].

The type of diversity used by JTIDS is the standard double-pulse structure (STDP) which corresponds to a sequential diversity of two. The same type of diversity is to be considered for the proposed waveform in this thesis for both AWGN only and an AWGN plus PNI environment.

For sequential diversity systems, if the bit rate is held constant as diversity L increases, then diversity effectively decreases the average energy per diversity transmission by a factor of L . On the other hand, if the average energy per diversity transmission is held constant as diversity L increases, then diversity effectively decreases the overall bit rate by a factor of L [6]. In this analysis the average energy per diversity transmission is considered constant since this reflects the way in which JTIDS is implemented. In effect, JTIDS transmits each pulse at a fixed power (presumably the maximum possible) so the double-pulse structure is equivalent to increasing the signal-to-noise ratio per symbol by 3 dB. In AWGN only, when compared on an average energy per bit basis, the performance of the double-pulse structure will be approximately the same or poorer (for noncoherent detection) than for the single-pulse structure. Any improvement obtained with the double-pulse structure will be seen when PNI is present, particularly when side information is used.

In this thesis we assume that our receiver employs soft decision demodulation since this demodulation technique is more amenable to the utilization of side information to reduce the effects of jamming.

1. Coherent Detection

The simplest case to analyze is coherent detection in an AWGN-only environment. For sequential diversity, L pulses are transmitted for every channel symbol. Since the transmitted pulses are received coherently and the AWGN is not affected by diversity, the received energy per symbol is L times the energy per pulse $E_s = LE_p$, or $E_s = rmLE_b$ where r is the code rate, m is the number of bits per symbol and E_b is the average bit energy per pulse. Hence, the probability of channel symbol error is obtained from equation (2.2) as

$$P_s = \frac{1}{\sqrt{2\pi}} \int_{-\infty}^{\infty} e^{\left(\frac{-u^2}{2}\right)} \left\{ 1 - \left[1 - Q\left(u + \sqrt{\frac{2LrmE_b}{N_0}}\right) \right]^{M-1} \right\} du . \quad (2.12)$$

On the other hand, in an AWGN plus PNI environment, when diversity of order L is employed and each diversity reception is independent of the others, the probability that i of L diversity receptions are affected by PNI, where ρ represents the fraction of time that the channel is affected by PNI, is [11]

$$\Pr(i, L) = \binom{L}{i} \rho^i (1 - \rho)^{L-i} \quad (2.13)$$

where $\binom{L}{i}$ are the number of distinct ways in which i out of L receptions can be received in error.

Consequently, the probability of channel symbol error is

$$P_s = \sum_{i=0}^L \left[\binom{L}{i} \rho^i (1 - \rho)^{L-i} P_s(i) \right] \quad (2.14)$$

where $P_s(i)$ is the conditional probability of channel symbol error given that i symbols experience PNI and $P_s(i)$ needs to be determined.

2. Noncoherent Detection

In order to derive the performance in AWGN for noncoherent detection of M -ary orthogonal modulation with L -fold sequential diversity and soft decision combining, we define $V_1, V_2 \dots V_M$ as the decision statistics for each diversity reception, where the respective probability density functions (pdfs) of the random variables prior to diversity combining are [6]

$$f_{V_{1_k}}(u_{1_k}/1) = \frac{1}{2\sigma^2} \exp\left[\frac{-(u_{1_k} + 2A_c^2)}{2\sigma^2}\right] I_0\left(\frac{A_c\sqrt{2u_{1_k}}}{\sigma^2}\right), \quad u_{1_k} \geq 0 \quad (2.15)$$

for the signal branch, assumed without loss of generality to be branch one, and

$$f_{V_{m_k}}(u_{m_k}/1) = \frac{1}{2\sigma^2} \exp\left(\frac{-u_{m_k}}{2\sigma^2}\right), \quad u_{m_k} \geq 0 \quad (2.16)$$

for the non-signal branch. These pdfs are chi-squared with two degrees of freedom, and $I_0(\bullet)$ is the modified Bessel function of the first kind and order zero.

The overall pdf for each branch of the receiver is derived by convolving the L individuals pdfs; hence, $f_{V_1}(u_1/1) = f_{V_{1_k}}^{\otimes L}(u_{1_k}/1)$ and $f_{V_m}(u_m/1) = f_{V_{m_k}}^{\otimes L}(u_{m_k}/1)$, which yields, respectively, [6]

$$f_{V_1}(u_1/1) = \frac{u_1^{(L-1)/2}}{2\sigma^2(2LA_c^2)^{(L-1)/2}} \times \exp\left[\frac{-(u_1 + 2LA_c^2)}{2\sigma^2}\right] I_{L-1}\left(\frac{A_c\sqrt{2Lu_1}}{\sigma^2}\right), \quad u_1 \geq 0 \quad (2.17)$$

and

$$f_{V_m}(u_m/1) = \frac{u_m^{L-1}}{(2\sigma^2)^{(L-1)!}} \exp\left(\frac{-u_m}{2\sigma^2}\right), \quad u_m \geq 0 \quad (2.18)$$

where $I_{L-1}(\bullet)$ is the modified Bessel function of the first kind and order $L-1$.

The probability of the channel symbol error is derived from

$$P_s = 1 - \Pr(V_1 > V_2 \cap V_1 > V_3 \cap \dots V_1 > V_M / 1) \quad (2.19)$$

which in this case is given by

$$P_s = 1 - \int_0^\infty f_{V_1}(u_1/1) \left[\int_0^{u_1} f_{V_m}(u_m/1) du_2 \right]^{M-1} du_1. \quad (2.20)$$

The derivation of performance in the case of an AWGN plus PNI environment is more complicated since there is a possibility that only some of the received pulses are affected by PNI. In this case the pdf for each variable must be determined taking into account the fact that for some pulses the noise power is $\sigma_0^2 = N_0/T_c$ while for others is $\sigma_T^2 = N_0/T_c + N_I/(\rho T_c)$. Consequently, the overall probability of channel symbol error P_s for a system which affected by PNI is

$$P_s = \sum_{i=0}^L \left[\binom{L}{i} \rho^i (1-\rho)^{L-i} P_s(i) \right] \quad (2.21)$$

where $P_s(i)$ is the conditional probability of channel symbol error given that i symbols experience PNI. For JTIDS, $L=2$, so equation (2.21) simplifies to

$$P_s = (1-\rho)^2 P_s(0) + 2\rho(1-\rho)P_s(1) + \rho^2 P_s(2) \quad (2.22)$$

where $P_s(0)$ is derived from equation (2.20) with $\sigma^2 = N_0/T_c$, whereas $P_s(2)$ is derived from equation (2.20) with $\sigma^2 = N_0/T_c + N_I/T_c$.

For the derivation of $P_s(1)$, the noise power for one pulse is $\sigma_0^2 = N_0/T_c$ and $\sigma_T^2 = N_0/T_c + N_I/\rho T_c$ for the other one. Hence, $f_{V_1}(u_1/1) = f_{V_k}^{\otimes 2}(u_k/1)$ is explicitly

$$f_{V_1}(u_1/1) = \int_0^{u_1} f_{V_{\sigma_0}}(\alpha) f_{V_{\sigma_T}}(u_1 - \alpha) d\alpha \quad (2.23)$$

or, from equation (2.15),

$$\begin{aligned} f_{V_1}(u_1/1) &= \int_0^{u_1} \frac{1}{4\sigma_0^2\sigma_T^2} \exp \left[\frac{-u_1}{2\sigma_T^2} - 2A_c^2 \left(\frac{1}{2\sigma_0^2} + \frac{1}{2\sigma_T^2} \right) \right] \\ &\times \exp \left[-\alpha \left(\frac{1}{2\sigma_0^2} + \frac{1}{2\sigma_T^2} \right) \right] I_0 \left(\frac{A_c \sqrt{2\alpha}}{\sigma_0} \right) I_0 \left(\frac{A_c \sqrt{2(u_1 - \alpha)}}{\sigma_T} \right) d\alpha \end{aligned} \quad (2.24)$$

which must be evaluated numerically.

For the $(M - 1)$ remaining branches of the receiver $f_{V_m}(u_m / 1) = f_{V_{m_k}}^{\otimes 2}(u_{m_k} / 1)$ can be evaluated analytically to obtain

$$f_{V_2}(u_2 / 1) = \frac{1}{2(\sigma_0^2 - \sigma_T^2)} \left(e^{\frac{-u_2}{2\sigma_0^2}} - e^{\frac{-u_2}{2\sigma_T^2}} \right), \quad u_2 \geq 0. \quad (2.25)$$

Using equations (2.20), (2.24), and (2.25), we can evaluate

$$P_s(1) = 1 - \int_0^\infty f_{V_1}(u_1 / 1) \left[\int_0^{u_1} f_{V_2}(u_2 / 1) du_2 \right]^{M-1} du_1 \quad (2.26)$$

Because of the complexity of equation (2.26) a numerical evaluation may be required rather an analytical one.

G. PERFECT-SIDE INFORMATION

For a system with a diversity of L , where the diversity receptions are received independently, perfect-side information (PSI) can be considered as a means to reduce to the effect of PNI. PSI is not realistic but provides a way to measure the relative effectiveness of practical side information. For a diversity of two, when both received symbols in the repetitive pulses are unaffected by PNI, they are combined and demodulated as usual. If either of the diversity receptions are affected by PNI, the receiver discards the PNI-affected symbol and makes a decision based on the remaining diversity reception affected only by AWGN. When both diversity receptions are affected by PNI, the receiver combines the two receptions and makes a decision. PSI requires at least a diversity of two and can improve system performance in a PNI environment where $\rho < 1$ [12].

H. CHAPTER SUMMARY

In this chapter, the background necessary to examine the performance of an alternative JTIDS/Link-16 waveform was introduced. In the next chapter, the performance analysis of the original JTIDS waveform is examined in order to use it as a reference for the proposed alternative waveform.

THIS PAGE INTENTIONALLY LEFT BLANK

III. PERFORMANCE ANALYSIS OF THE ORIGINAL JTIDS WAVEFORM

In this chapter, we examine the performance of the original JTIDS waveform. The results of this chapter can be used for comparison with the performance of the proposed waveform.

We first examine the performance for coherent demodulation in both AWGN only and an AWGN plus PNI environment. Second the performance of the original JTIDS waveform for noncoherent demodulation in both AWGN and AWGN plus PNI is examined. The JTIDS/Link-16 message data can be sent with either a single-pulse structure or a double-pulse structure. In this thesis, only the single-pulse structure is analyzed.

A. BRIEF DESCRIPTION OF A JTIDS/LINK-16-TYPE SYSTEM

JTIDS features RS coding, symbol interleaving, CCSK for M -ary baseband symbol modulation, MSK chip modulation for transmission, single-pulse or double-pulse diversity, and combined frequency-hopped and direct sequence (FH/DS) spread spectrum for transmission security. Based on [13], [14], and [15], the physical layer (or transceiver) of a JTIDS-type system is illustrated in Figure 2.

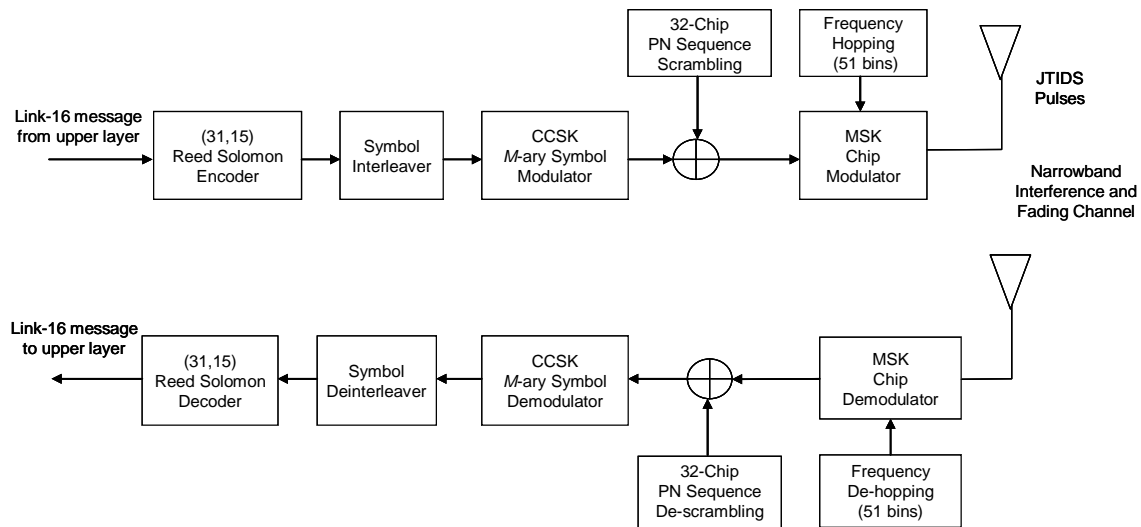


Figure 2. A JTIDS/Link-16-type system model. From [4]

The performance analysis of the original JTIDS waveform uses the conditional probabilities of symbol error for the 32-chip CCSK sequence derived in [4]. In Table 1, the conditional probabilities ζ_{UB_j} for N chip errors ($0 \leq N \leq 32$) are listed.

Table 1. Conditional probabilities of symbol error for the 32-chip CCSK sequence chosen for JTIDS. From [4]

$N = j$	ζ_{UB_j}
0	0
1	0
\vdots	\vdots
6	0
7	0.0015
8	0.0207
9	0.1166
10	0.4187
11	1.0
12	1.0
\vdots	\vdots
32	1.0

B. COHERENT DEMODULATION

1. AWGN Only Environment

The probability of symbol error for the 32-chip CCSK sequence chosen for the JTIDS is [4]

$$P_s = \sum_{j=0}^{32} \zeta_j \binom{32}{j} P_c^j (1 - P_c)^{32-j} \quad (3.1)$$

where ζ_j are the conditional probabilities of symbol error for CCSK, and P_c is the probability of chip error at the output of the MSK chip demodulator. If we use ζ_{UB_j} in equation (3.1), then an analytic upper bound on the probability of symbol error for the 32-chip CCSK sequence chosen for JTIDS is given by [4]

$$P_s < \sum_{j=0}^{32} \zeta_{UB_j} \binom{32}{j} P_c^j (1 - P_c)^{32-j} . \quad (3.2)$$

MSK can be considered as a special case of offset quadrature phase-shift keying with sinusoidal pulse shaping. When a coherent matched filter or correlator is used to recover the chips, MSK has the same performance as BPSK, QPSK and OQPSK [4]; hence, since $E_c = 5rE_b / 32$,

$$P_c = Q\left(\sqrt{\frac{10rE_b}{32N_0}}\right) \quad (3.3)$$

where for the Reed-Solomon code used for JTIDS $r=15/31$.

Combining equations (2.8), (3.2) and (3.3), we obtain the probability of symbol error of the original JTIDS waveform in AWGN environment. To obtain the respective probability of bit error we must evaluate

$$P_b \approx \frac{m+1}{2m} P_s \quad (3.4)$$

The result is shown in Figure 3. As it can be seen, the E_b / N_0 required for relatively reliable communication ($P_s = 10^{-5}$) is 7dB.

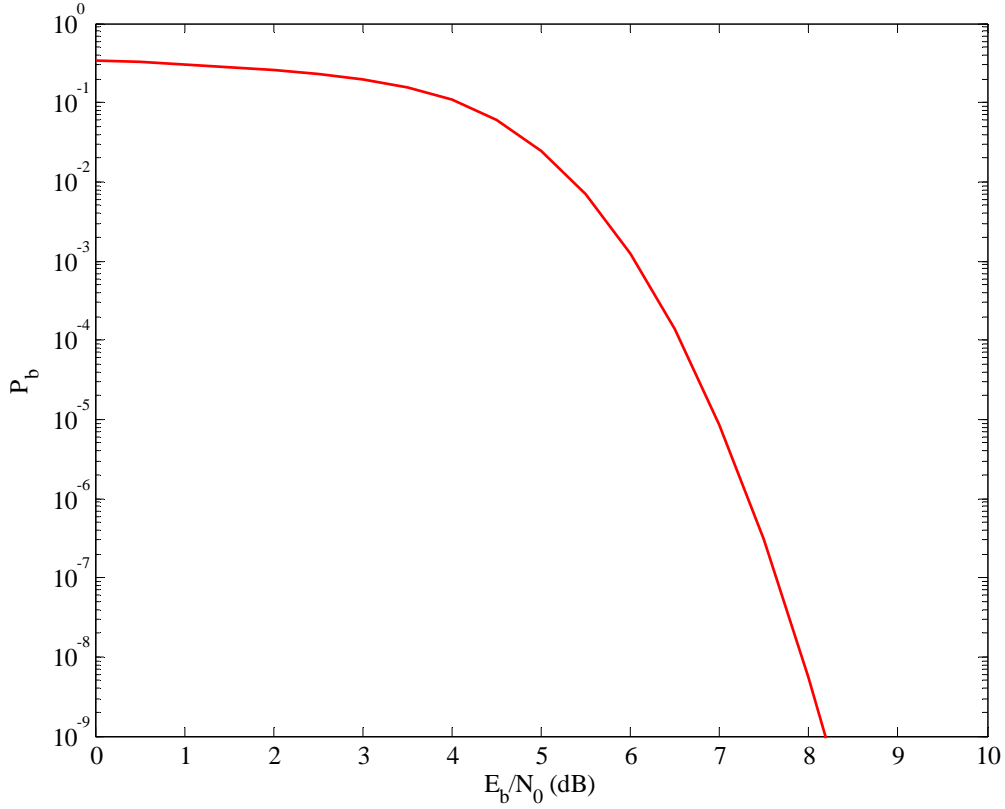


Figure 3. Performance of the JTIDS waveform in AWGN only environment and coherent demodulation.

2. AWGN Plus PNI Environment

When the original JTIDS waveform experiences both AWGN and PNI, the probability of channel symbol error P_s is [4]

$$P_s = \rho P_s'' + (1 - \rho) P_s' \quad (3.5)$$

where P_s'' is the probability of channel symbol error with PNI and P_s' is the probability of channel symbol error without PNI. The P_s' is obtained from equations (3.2) and (3.3), whereas the P_s'' is derived by equation (3.2) with [4]

$$P_c = Q \left(\sqrt{\frac{10rE_b}{32(N_0 + N_I / \rho)}} \right). \quad (3.6)$$

Combining equations (2.8), (3.2), (3.4), (3.5), and (3.6), we obtain the probability of bit error for the original JTIDS waveform in AWGN plus PNI. The results are shown in Figure 4 for $E_b / N_0 = 10$ dB and several values of ρ .

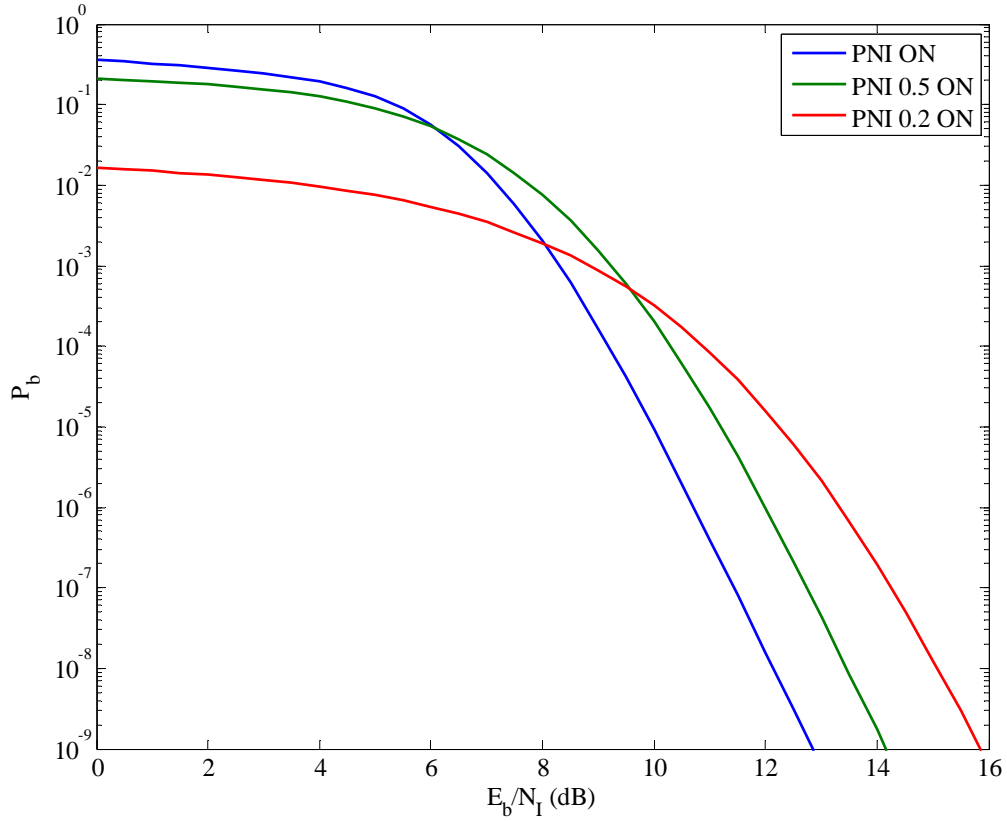


Figure 4. Performance of the JTIDS waveform in an AWGN plus PNI environment and coherent demodulation for $E_b / N_0 = 10$ dB with $\rho = 1$, $\rho = 0.5$, and $\rho = 0.2$.

C. NONCOHERENT DEMODULATION

1. AWGN Only Environment

For noncoherent demodulation in AWGN, all the equations used for coherent demodulation still hold except for P_c , which becomes [3]

$$P_c = \exp\left(\frac{-10rE_b}{32N_0}\right). \quad (3.7)$$

The probability of channel bit error obtained is shown in Figure 5.

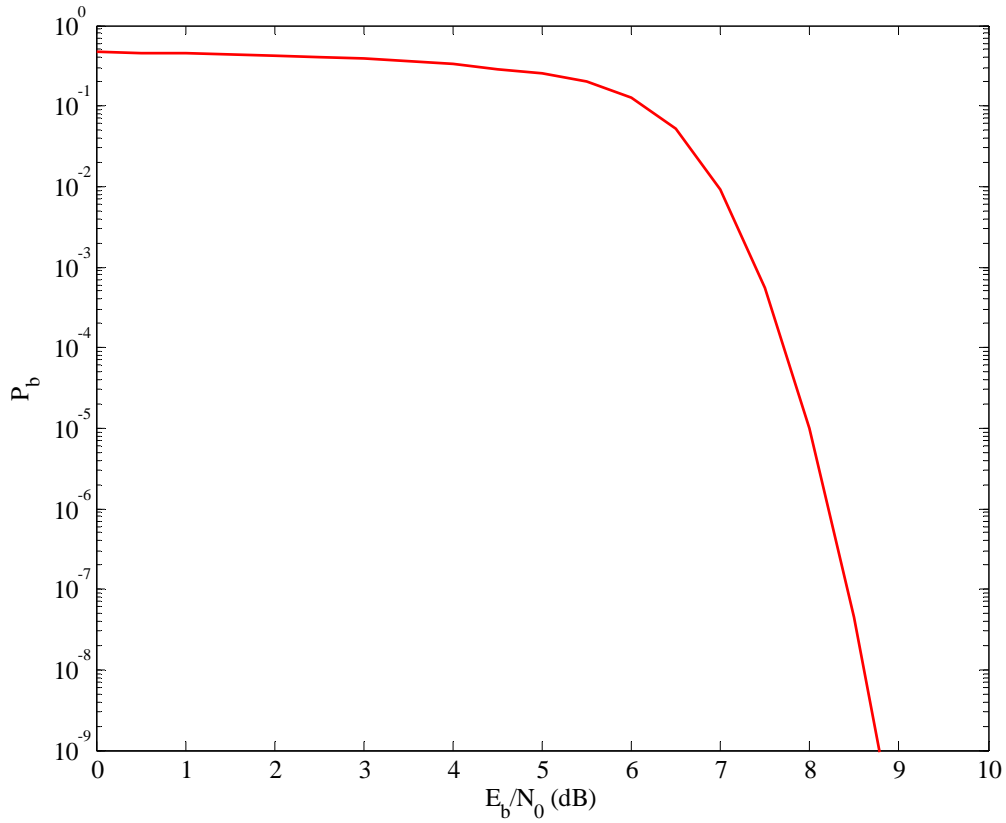


Figure 5. Performance of JTIDS with noncoherent demodulation in AWGN.

2. AWGN Plus PNI Environment

Likewise, all the equations used for the coherent case still hold except for equation (3.6), which is replaced by [3]

$$P_c = \frac{1}{2} \exp\left(\frac{-10rE_b}{32(N_0 + N_I / \rho)}\right). \quad (3.8)$$

The results obtained are shown in Figure 6 for $E_b / N_0 = 10$ dB and several values of ρ .

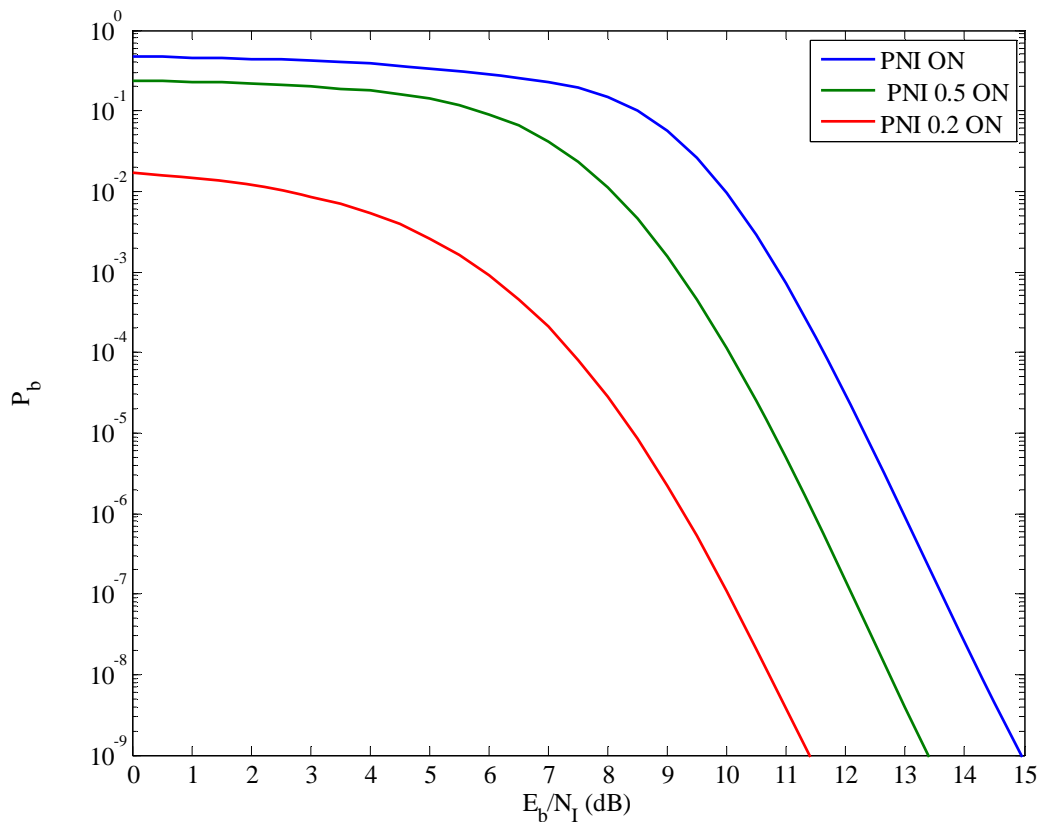


Figure 6. Performance of JTIDS with noncoherent demodulation for $E_b / N_0 = 10$ dB with $\rho = 1$, $\rho = 0.5$, and $\rho = 0.2$.

D. CHAPTER SUMMARY

In this chapter, the performance of the original JTIDS/Link-16 waveform for both coherent and noncoherent demodulation was examined. In the next chapter, we will determine the optimum k of the Reed-Solomon $(31, k)$ code which yields the best performance for the alternative waveform, and the results will be compared with the original JTIDS.

THIS PAGE INTENTIONALLY LEFT BLANK

IV. PERFORMANCE ANALYSIS OF COHERENT AND NONCOHERENT ORTHOGONAL SIGNALING FOR A CONVOLUTIONAL CODE CONCATENATED WITH A RS CODE IN AWGN

In this chapter, the performance of the alternative waveform in an AWGN only environment for both coherent and noncoherent demodulation is analyzed. In addition, the optimum k for the $(31, k)$ RS code needed to obtain the minimum probability of bit error at the output of the receiver is determined.

A. COHERENT DEMODULATION

The encoding and decoding configuration of the proposed JTIDS-type system is shown in Figure 1 and is reproduced here for convenience.

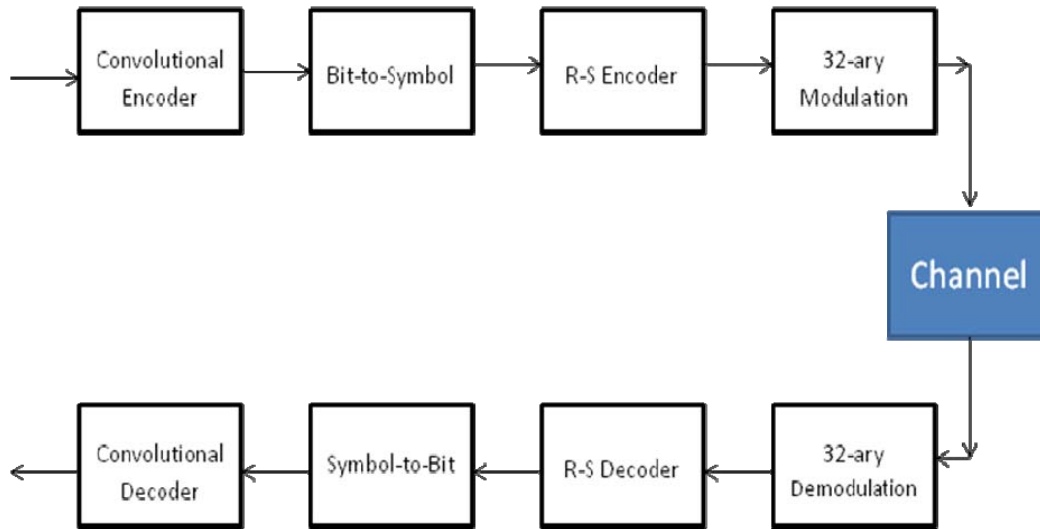


Figure 7. Encoding and decoding configuration of the proposed system.

In order to obtain the overall probability of bit error at the receivers output we must first find the probability of channel symbol error at the output of the 32-ary demodulator. For the coherent case in an AWGN environment with two-sided noise power spectral density $N_0 / 2$, the probability of channel symbol error expressed in terms of symbol energy is obtained from equation (2.1). Expressed in terms of bit energy E_b , (2.1) is given by

$$P_s \leq (M - 1)Q\left(\sqrt{\frac{rmE_b}{N_0}}\right) \quad (4.1)$$

where r is the overall code rate of the concatenated code and is the product of the individual code rates of the convolutional (4/5) and the RS ($k/31$) code.

The upper bound given by equation (4.1) combined with equation (2.8) yields the probability of symbol error P_s at the output of the (31, k) RS decoder. Using this result, we obtain the probability of bit error at the symbol-to-bit converter output by taking the average value of the upper and lower bound on the probability of bit error given that a symbol error has occurred to get

$$P_b = 0.5\left(1 + \frac{1}{5}\right)P_s = 0.6P_s \quad (4.2)$$

The overall probability of bit error at the output of the receiver is obtained from equations (2.8), (2.9), (2.10), (2.11), (4.1) and (4.2) in the form of a very tight upper bound.

The performance of the alternative waveform for six possible values of k as well as the performance of the original JTIDS/Link-16 waveform for coherent demodulation in an AWGN environment are shown in Figure 8. We observe that the proposed waveform performs much better than the original JTIDS waveform. In addition, we observe that the optimum rate for the Reed-Solomon code is 25/31 ($k=25$). Hence, from equation (2.7), the throughput of the proposed system is 33% better than the existing JTIDS/Link-16 waveform.

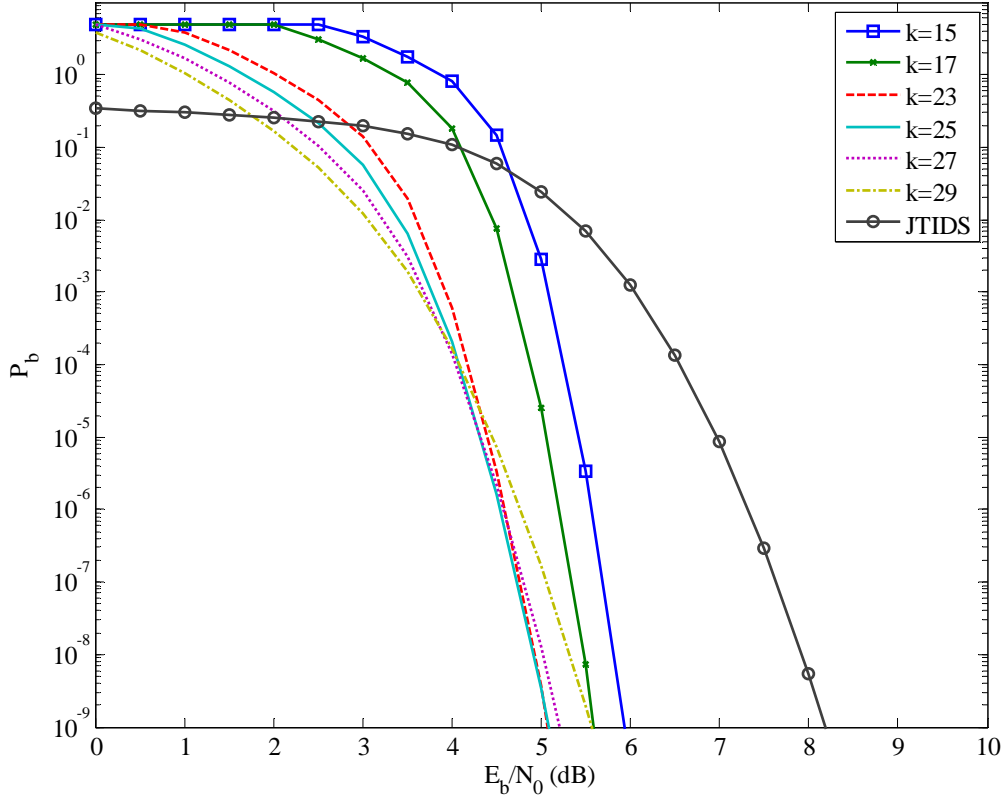


Figure 8. Performance of the alternative waveform with coherent demodulation in AWGN.

B. NONCOHERENT DEMODULATION

As discussed in Chapter II, the probability of channel symbol error for orthogonal signaling with baseband waveforms with noncoherent demodulation is upper bounded by

$$P_s \leq \frac{M-1}{2} \exp\left(\frac{-rE_s}{2N_0}\right) \quad (4.3)$$

which, expressed in terms of bit energy, is given by

$$P_s \leq \frac{M-1}{2} \exp\left(\frac{-rmE_b}{2N_0}\right) \quad (4.4)$$

As for coherent demodulation, the probability of bit error is obtained from equations (2.8), (2.9), (2.10), (4.2), (4.4), and (2.11). More specifically, by substituting equation (4.4) into (2.8), we obtain the probability of symbol error at the output of the

(31, k) RS decoder. The probability of bit error at the input of the (4/5) convolutional decoder is obtained from equation (4.2), which is then used in equations (2.9), (2.10), and (2.11) to derive the overall probability of bit error of the system.

From the results illustrated in Figure 9, we observe that the proposed waveform performs better than the original JTIDS waveform in an AWGN only environment with noncoherent demodulation. In addition we observe that the optimum code rate for the Reed-Solomon code for this case is again 25/31 ($k=25$).

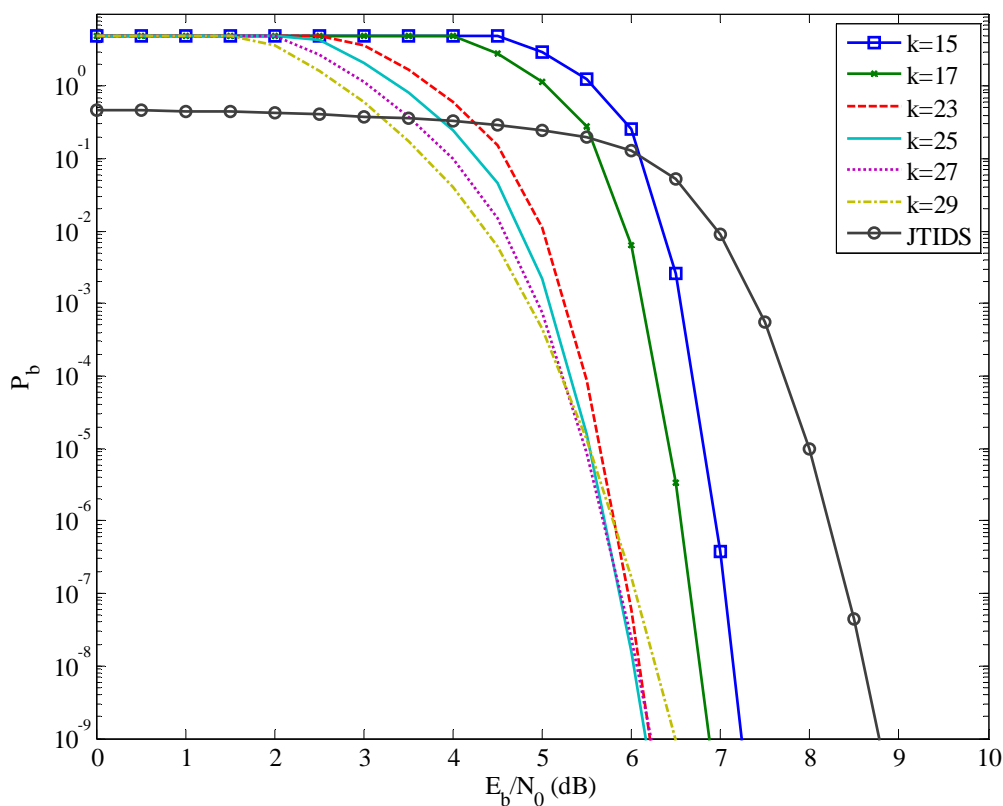


Figure 9. Performance of the alternative waveform with noncoherent demodulation in AWGN.

C. COMPARISON BETWEEN COHERENT AND NONCOHERENT DEMODULATION FOR THE ALTERNATIVE WAVEFORM

For purposes of comparison, the performance obtained for both coherent and noncoherent demodulation of the alternative waveform in AWGN is plotted in Figure 10 for $k=25$, which earlier in this chapter was shown to yield the best results for both types of demodulation.

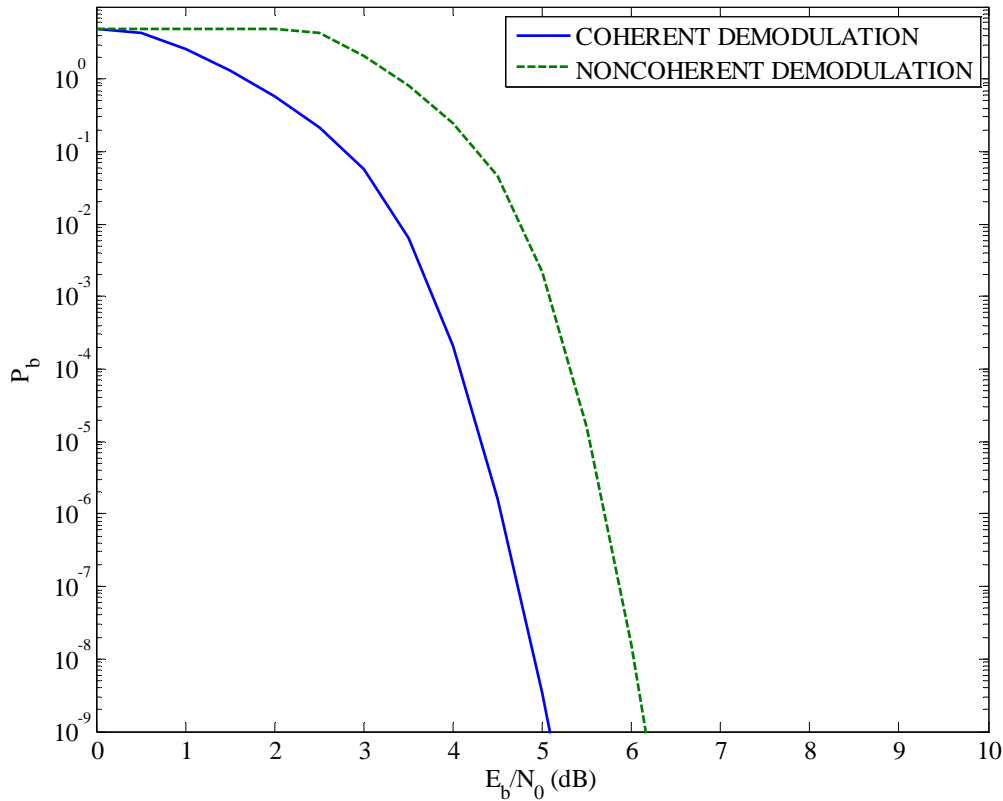


Figure 10. Comparison of the performance of the coherent and noncoherent demodulation for the proposed waveform in AWGN.

From Figure 10, we observe that the alternative waveform with coherent demodulation performs better than the one with noncoherent demodulation. Indeed, in Table 2 we see that when $P_b = 10^{-5}$, the proposed waveform requires $E_b / N_0 = 4.2$ dB for coherent demodulation, whereas for noncoherent $E_b / N_0 = 5.5$ dB is needed.

Table 2. Comparison of the performance of the alternative waveform for coherent and noncoherent demodulation when $P_b = 10^{-5}$ in AWGN.

Demodulation	P_b	E_b / N_0 (dB)
Coherent	10^{-5}	4.2
Noncoherent	10^{-5}	5.5

D. CHAPTER SUMMARY

In this chapter, the performance of the alternative waveform in an AWGN only environment was investigated for both coherent and noncoherent demodulation. The results were compared to those of the existing JTIDS/Link-16 waveform. In addition, the optimum k for the $(31, k)$ RS was determined to be 25 for both the coherent and the noncoherent case. In the next chapter, the performance of the proposed waveform in an AWGN plus PNI environment for both coherent and noncoherent demodulation is investigated.

V. PERFORMANCE ANALYSIS OF COHERENT AND NONCOHERENT ORTHOGONAL SIGNALING WITH A CONVOLUTIONAL CODE CONCATENATED WITH A RS CODE IN AWGN AND PNI

In this chapter, the performance of the alternative waveform in AWGN and PNI for both coherent and noncoherent demodulation is analyzed. Only the (31, 25) RS code is considered.

With PNI, we assume that the communications system is attacked by a noise like signal that is turned on and off randomly. If ρ represents the fraction of time that the PNI is turned on, then $(1-\rho)$ represents the fraction of time that the PNI is turned off where $0 < \rho \leq 1$. In this kind of noisy environment, received symbols are affected by two different levels of noise power since some of the symbols are affected only by AWGN and others by both AWGN and PNI. If the one-sided power spectral density (PSD) of the AWGN is N_0 and the one-sided PSD of barrage noise interference is N_I , then N_I / ρ is the PSD of the PNI since we assume that the average interference power is independent of ρ [3].

A. COHERENT DEMODULATION

The derivation of the probability of bit error of the alternative waveform in an AWGN plus PNI environment is very similar to the one previously obtained for the AWGN only case with coherent demodulation. The only significant difference is that the transmitted signal now is affected differently by the channel and, thus, the probability of symbol error at the demodulator output is changed. As mentioned in Chapter II, equation (2.2) must be used instead of equation (2.1) because the accuracy provided by the union bound does not suffice in this case. In addition, the overall probability of channel symbol error is a combination of symbols, some of which are affected by PNI and some which are not. Consequently, combining equations (2.2), (2.5) and (2.6), we obtain

$$\begin{aligned}
P_s &= \rho \frac{1}{\sqrt{2\pi}} \int_{-\infty}^{\infty} e^{\left(\frac{-u^2}{2}\right)} \left\{ 1 - \left[1 - Q \left(u + \sqrt{\frac{2rE_s}{N_0 + N_I / \rho}} \right) \right]^{M-1} \right\} du \\
&+ (1-\rho) \frac{1}{\sqrt{2\pi}} \int_{-\infty}^{\infty} e^{\left(\frac{-u^2}{2}\right)} \left\{ 1 - \left[1 - Q \left(u + \sqrt{\frac{2rE_s}{N_0}} \right) \right]^{M-1} \right\} du
\end{aligned} \tag{5.1}$$

which in terms of bit energy can be written as

$$\begin{aligned}
P_s &= \rho \frac{1}{\sqrt{2\pi}} \int_{-\infty}^{\infty} e^{\left(\frac{-u^2}{2}\right)} \left\{ 1 - \left[1 - Q \left(u + \sqrt{\frac{2rm}{\frac{N_0}{E_b} + \frac{N_I}{\rho E_b}}} \right) \right]^{M-1} \right\} du \\
&+ (1-\rho) \frac{1}{\sqrt{2\pi}} \int_{-\infty}^{\infty} e^{\left(\frac{-u^2}{2}\right)} \left\{ 1 - \left[1 - Q \left(u + \sqrt{\frac{2rmE_b}{N_0}} \right) \right]^{M-1} \right\} du
\end{aligned} \tag{5.2}$$

Combining equations (2.8), (4.2), (5.2) and (2.11), we derive the overall probability of bit error for the proposed waveform in AWGN and PNI with coherent demodulation. The performance of the alternative waveform for different values of ρ when $E_b / N_0 = 4.7\text{dB}$ is shown in Figure 11. An $E_b / N_0 = 4.7\text{ dB}$ is chosen because the probability of information bit error of the alternative waveform asymptotically approaches 10^{-8} for $E_b / N_I \gg 1$.

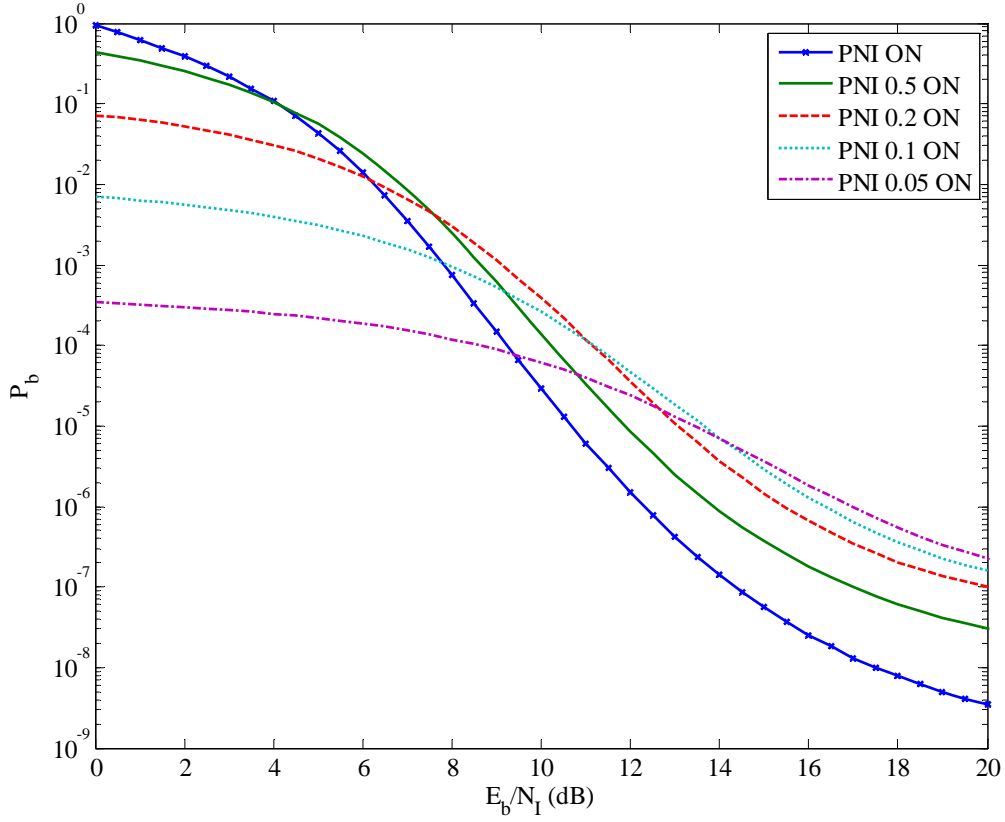


Figure 11. Performance of the proposed waveform in both AWGN and PNI with coherent demodulation for $\rho = 1$, $\rho = 0.5$, $\rho = 0.2$, $\rho = 0.1$ and $\rho = 0.05$ when $E_b / N_0 = 4.7$ dB.

From Figure 11, we observe that the PNI degrades the performance of the alternative waveform significantly. More specifically, as the fraction of time where the PNI is on is reduced, the performance of the system degrades more for $E_b / N_1 \gg 1$. However, for ρ smaller than 0.05, the performance of the system is not effectively degraded because the maximum probability of error drops into the range where reliable data communications can be achieved ($P_b < 10^{-5}$).

The performance of the existing JTIDS/Link-16 waveform for coherent demodulation when $E_b / N_0 = 4.7$ dB for different values of ρ is presented in Figure 12.

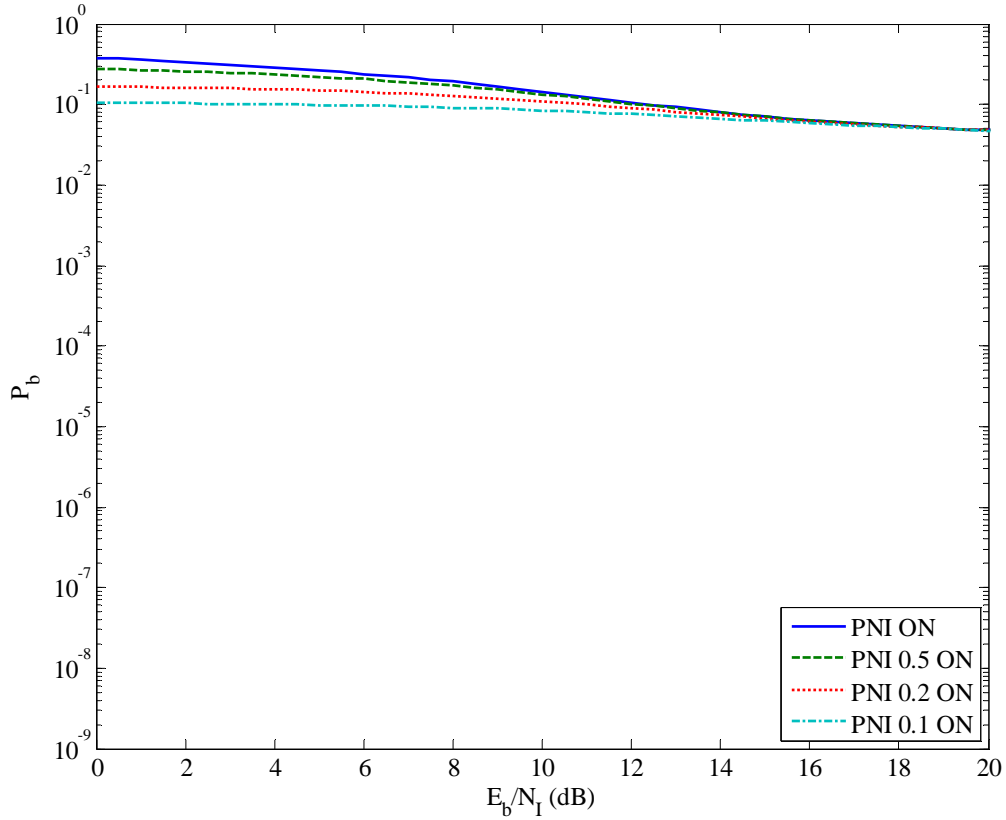


Figure 12. Performance of the original JTIDS/Link-16 waveform in both AWGN and PNI with coherent demodulation for $\rho = 1$, $\rho = 0.5$, $\rho = 0.2$ and $\rho = 0.1$ when $E_b / N_0 = 4.7$ dB.

Comparing Figures 11 and 12, we observe that the performance of the alternative waveform is superior to that of the original JTIDS/Link-16 when the bit energy-to noise power spectral density is small. In fact, from Figure 12, we see that reliable communication is not possible for the existing JTIDS/Link-16 when $E_b / N_0 = 4.7$ dB regardless of E_b / N_1 and ρ .

The performance of the proposed and the existing JTIDS/Link-16 waveforms when $E_b / N_0 = 8.4\text{dB}$ is presented in Figure 13 and Figure 14, respectively, in order to make the comparison for a larger value of E_b / N_0 for completeness.

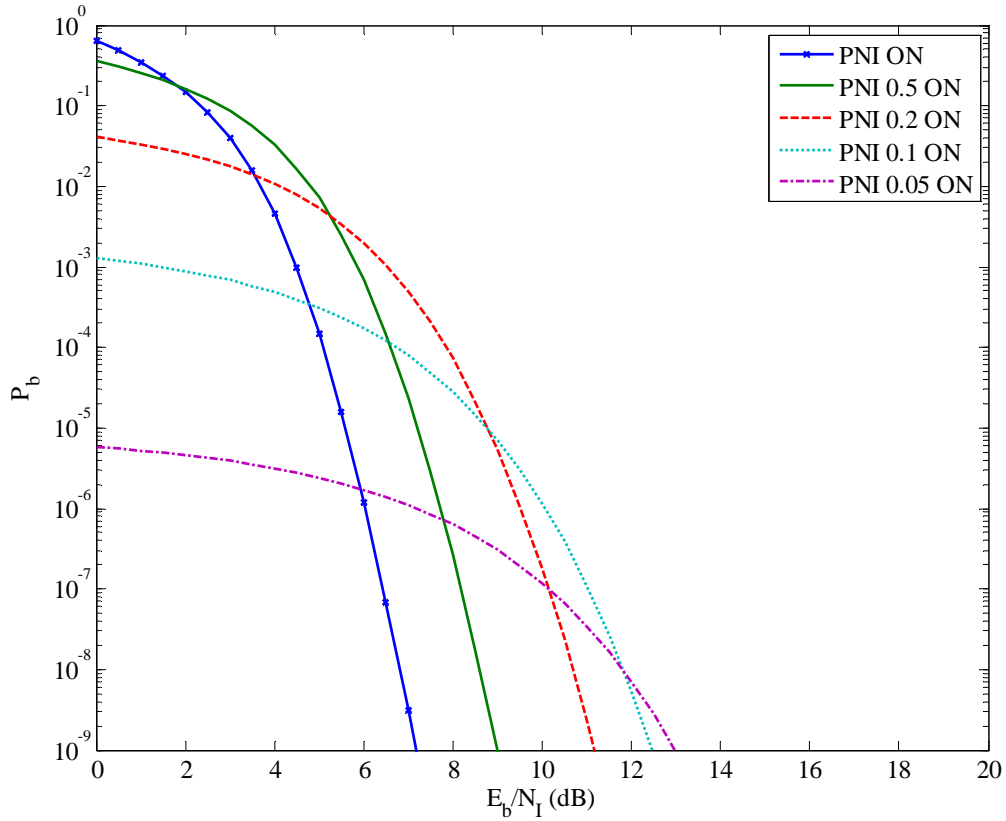


Figure 13. Performance of the alternative waveform in both AWGN and PNI with coherent demodulation for $\rho = 1, \rho = 0.5, \rho = 0.2, \rho = 0.1, \text{ and } \rho = 0.05$ when $E_b / N_0 = 8.4\text{dB}$.

From Figure 13, we see that in this case also PNI degrades the performance of the alternative waveform significantly. As mentioned previously, as the fraction of time where the PNI is on is reduced, the performance of the system degrades too. For $\rho \leq 0.1$, performance is not affected significantly and $P_b < 10^{-5}$.

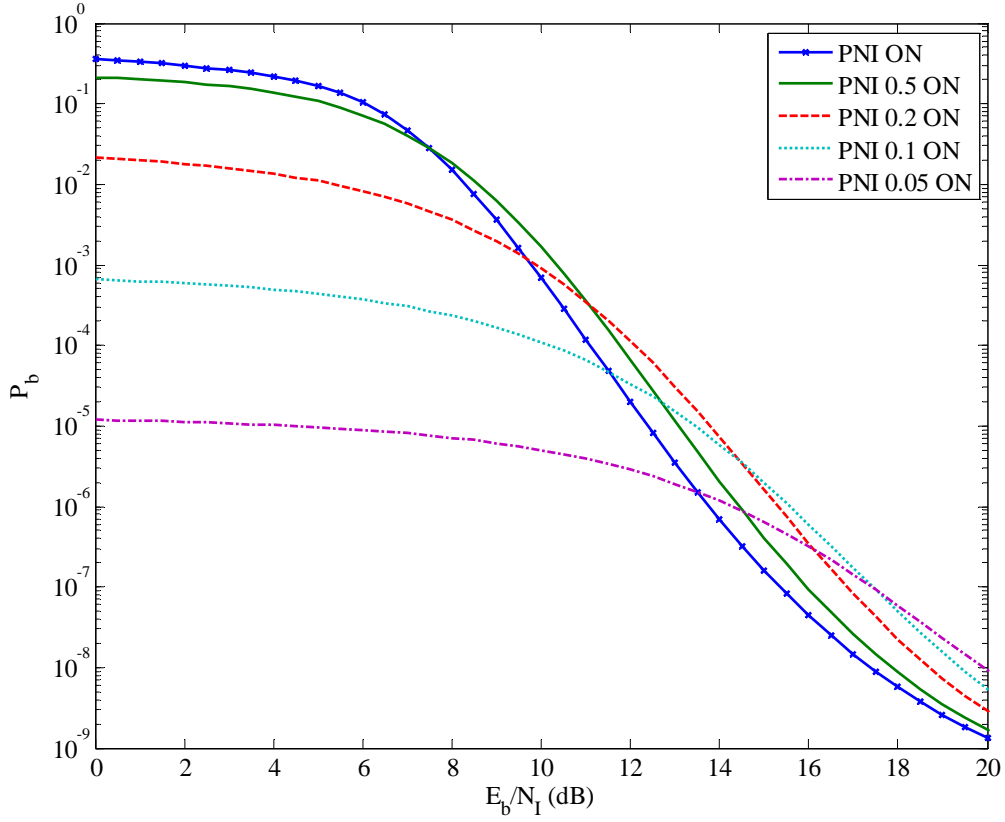


Figure 14. Performance of the original JTIDS/Link-16 waveform in both AWGN and PNI with coherent demodulation for $\rho = 1$, $\rho = 0.5$, $\rho = 0.2$, $\rho = 0.1$, and $\rho = 0.05$ when $E_b / N_0 = 8.4$ dB.

Comparing Figures 13 and 14, we observe that the performance of the alternative waveform is again superior to that of the existing JTIDS/Link-16. In order to illustrate the differences between the two waveforms, the specific values of E_b / N_f in dB for which the probability of bit error set as a reference for reliable communications ($P_b = 10^{-5}$) is met are presented in Table 3 and Table 4 for $E_b / N_0 = 4.7$ dB and $E_b / N_0 = 8.4$ dB, respectively.

Table 3. Comparison of the performance of the original JTIDS/Link-16 and the alternative waveforms for different values of ρ for coherent demodulation when $E_b / N_0 = 4.7$ dB.

P_b	ρ	E_b / N_1 (dB)	E_b / N_1 (dB)
		Original JTIDS	Proposed Waveform
10^{-5}	1	\emptyset	10.5
10^{-5}	0.5	\emptyset	11.9
10^{-5}	0.2	\emptyset	13
10^{-5}	0.1	\emptyset	13.5
10^{-5}	0.05	\emptyset	13.6

From Table 3, we can see that PNI with $\rho = 0.05$ degrades the performance of the alternative waveform relative to barrage noise interference (BNI) when $P_b = 10^{-5}$ and $E_b / N_0 = 4.7$ dB by 3.1 dB, whereas the original JTIDS/Link-16 cannot reach this probability of bit error at all.

Table 4. Comparison of the performance of the original JTIDS/Link-16 and the alternative waveforms for different values of ρ for coherent demodulation when $E_b / N_0 = 8.4$ dB.

P_b	ρ	E_b / N_t (dB)	E_b / N_t (dB)
		Original JTIDS	Proposed Waveform
10^{-5}	1	12.5	5.6
10^{-5}	0.5	13.1	7.2
10^{-5}	0.2	13.7	8.8
10^{-5}	0.1	13.4	8.8
10^{-5}	0.05	\emptyset	\emptyset

From Table 4, we observe that for any value of ρ the alternative waveform performs significantly better than the existing JTIDS/Link-16. As mentioned in Chapter III, this improvement in required received signal power comes with a 33% increase in throughput, where the increase is given by equation (2.7). From Table 4 we also can see that PNI with $\rho = 0.1$ degrades the performance of the proposed system relative to BNI when $P_b = 10^{-5}$ and $E_b / N_0 = 8.4$ dB by 3.2 dB, whereas the existing JTIDS/Link-16 performance is degraded by 1.2 dB. In addition, we see that both the alternative waveform and the existing JTIDS/Link-16 waveform are not significantly corrupted by PNI when $\rho \leq 0.1$.

B. NONCOHERENT DEMODULATION

When AWGN and PNI are both present, the probability of channel symbol error for 32-ary orthogonal signaling with noncoherent demodulation is obtained by combining equations (2.4), (2.5) and (2.6) to get

$$\begin{aligned}
P_s &= \rho \sum_{n=1}^{M-1} \frac{(-1)^{n+1}}{n+1} \binom{M-1}{n} \exp \left[\frac{-nrE_s}{(n+1)(N_0 + N_I / \rho)} \right] \\
&+ (1-\rho) \sum_{n=1}^{M-1} \frac{(-1)^{n+1}}{n+1} \binom{M-1}{n} \exp \left[\frac{-nrE_s}{(n+1)N_0} \right]
\end{aligned} \tag{5.3}$$

Which, in terms of bit energy can be written as

$$\begin{aligned}
P_s &= \rho \sum_{n=1}^{M-1} \frac{(-1)^{n+1}}{n+1} \binom{M-1}{n} \exp \left[\frac{-nrm}{(n+1) \left(\frac{N_0}{E_b} + \frac{N_I}{\rho E_b} \right)} \right] \\
&+ (1-\rho) \sum_{n=1}^{M-1} \frac{(-1)^{n+1}}{n+1} \binom{M-1}{n} \exp \left[\frac{-nrmE_b}{(n+1)N_0} \right].
\end{aligned} \tag{5.4}$$

Combining equations (2.8), (4.2), (5.4) and (2.11), we obtain the overall probability of bit error for the proposed waveform in an AWGN plus PNI environment with noncoherent demodulation. The performance of the alternative waveform for different values of ρ when $E_b / N_0 = 6$ dB is shown in Figure 15. An $E_b / N_0 = 6$ dB is chosen because the probability of information bit error of the alternative waveform asymptotically approaches a value where very reliable communication can be achieved for $E_b / N_I \gg 1$.

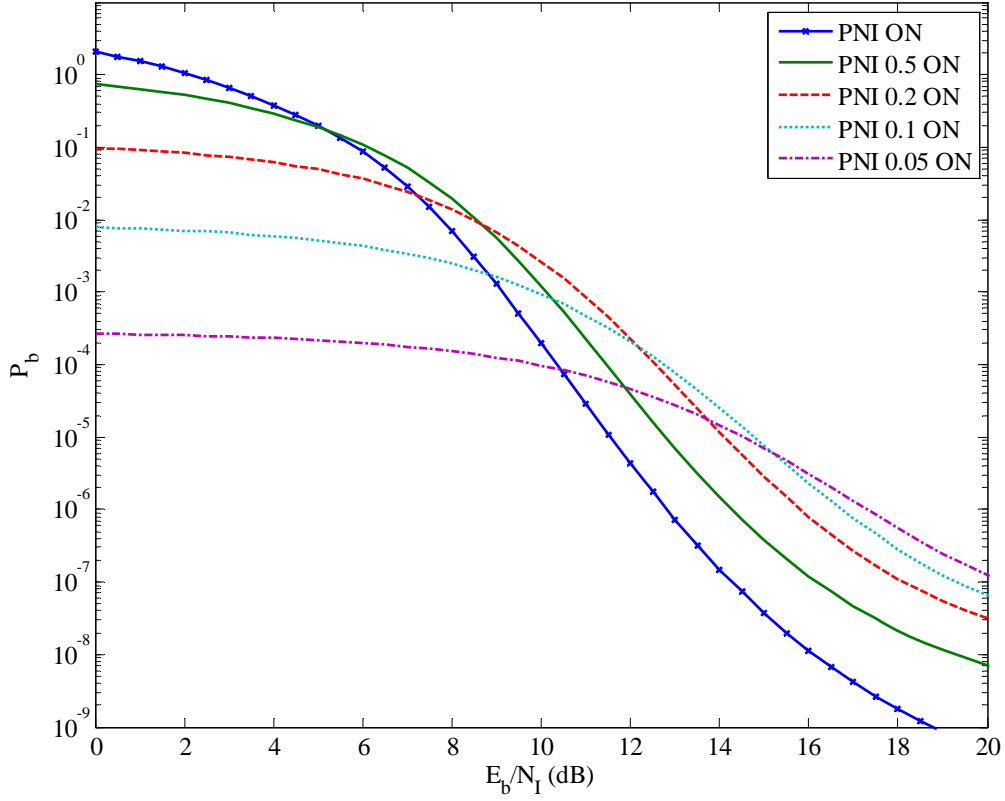


Figure 15. Performance of the alternative waveform in both AWGN and PNI with noncoherent demodulation for $\rho = 1$, $\rho = 0.5$, $\rho = 0.2$, $\rho = 0.1$, and $\rho = 0.05$ when $E_b / N_0 = 6$ dB.

From Figure 15, we observe that the PNI degrades the performance of the alternative waveform significantly. Indeed as the fraction of time where PNI is on is reduced the performance of the system degrades too. However, for $\rho \leq 0.05$ the performance of the system is not affected by PNI for $P_b \geq 10^{-5}$.

The performance of the existing JTIDS/Link-16 waveform for noncoherent demodulation when $E_b / N_0 = 6$ dB for different values of ρ is presented in Figure 16.

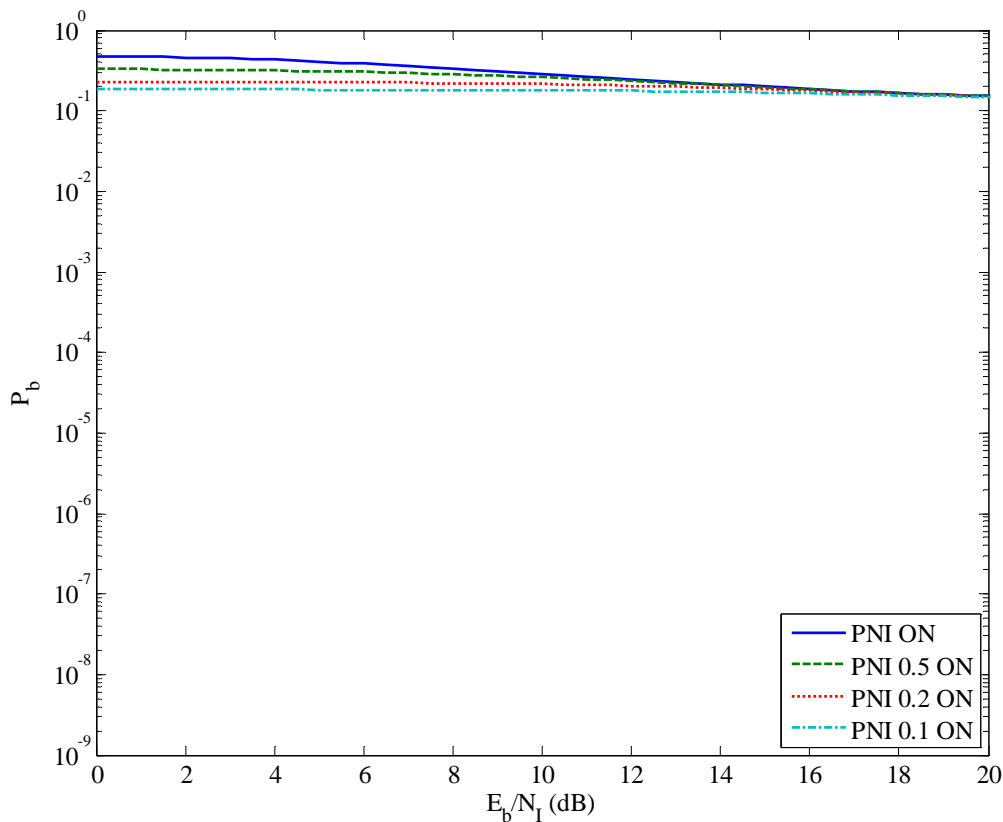


Figure 16. Performance of the original JTIDS/Link-16 waveform in both AWGN and PNI with noncoherent demodulation for $\rho = 1$, $\rho = 0.5$, $\rho = 0.2$ and $\rho = 0.1$ when $E_b / N_0 = 6$ dB.

Comparing Figures 15 and 16, we observe that the performance of the alternative waveform is superior to that of the original JTIDS/Link-16 when the bit energy-to noise power spectral density is small. In fact, from Figure 16, we see that reliable communication is not possible for the existing JTIDS/Link-16 when $E_b / N_0 = 6$ dB for any value of E_b / N_f and ρ .

The performance of the proposed and the existing JTIDS/Link-16 waveforms when $E_b / N_0 = 8.4$ dB is presented in Figure 17 and Figure 18, respectively.

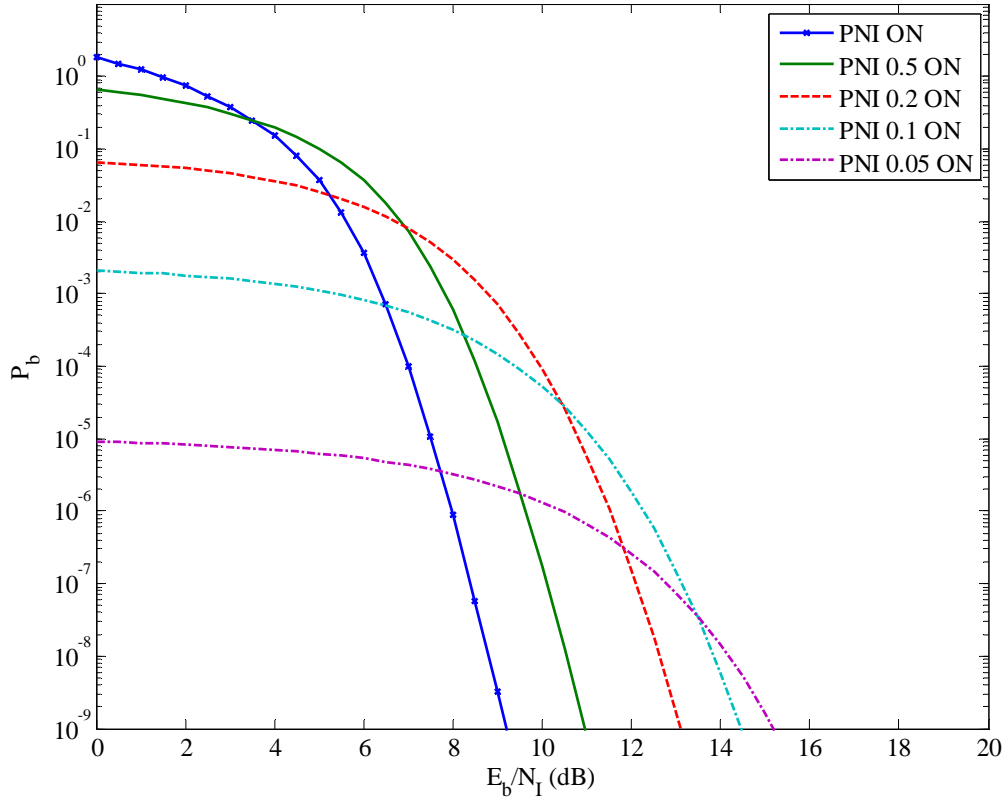


Figure 17. Performance of the alternative waveform in both AWGN and PNI with noncoherent demodulation for $\rho = 1$, $\rho = 0.5$, $\rho = 0.2$, $\rho = 0.1$, and $\rho = 0.05$ when $E_b / N_0 = 8.4$ dB.

From Figure 17 we see that, in this case also, PNI degrades the performance of the alternative waveform significantly. As mentioned previously, as the fraction of time where the PNI is on is reduced, the performance of the system degrades. For $\rho \leq 0.1$, $P_b \leq 10^{-5}$ for all E_b / N_1 .

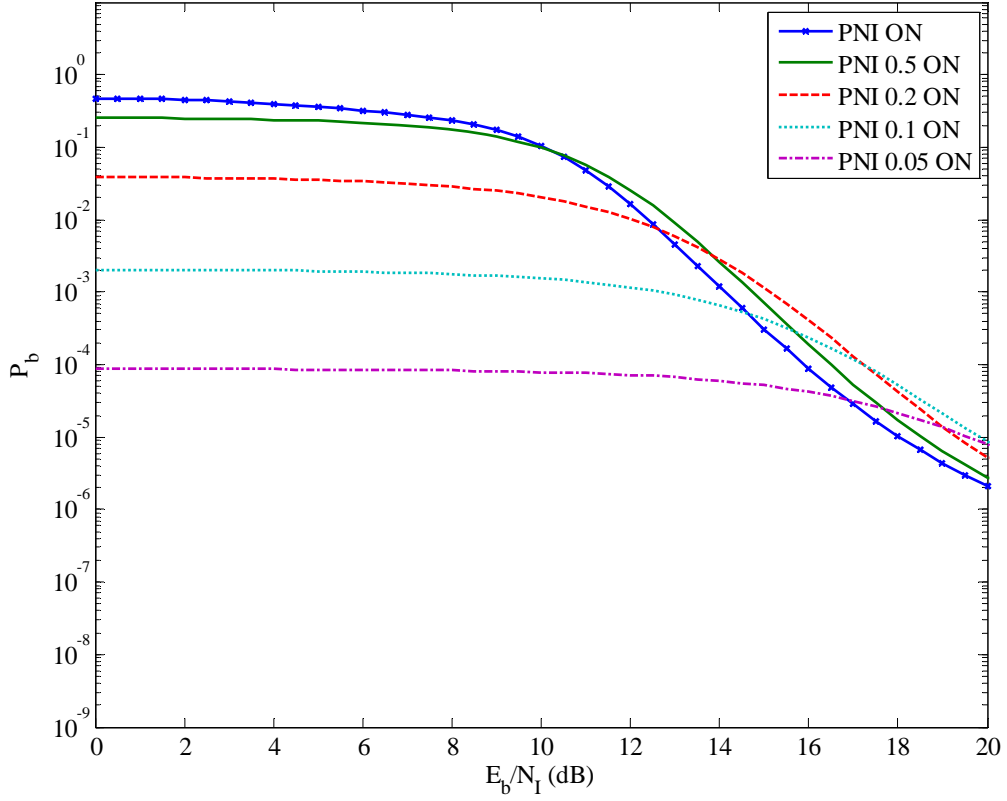


Figure 18. Performance of the original JTIDS/Link-16 waveform in both AWGN and PNI with noncoherent demodulation for $\rho = 1$, $\rho = 0.5$, $\rho = 0.2$, $\rho = 0.1$, and $\rho = 0.05$ when $E_b / N_0 = 8.4$ dB.

Comparing Figures 17 and 18, we observe that the performance of the alternative waveform is superior to that of the existing JTIDS/Link-16 again. In order to illustrate the differences between the two waveforms, the specific values of E_b / N_1 in dB for $P_b = 10^{-5}$ are presented in Table 5 and Table 6 for $E_b / N_0 = 6$ dB and $E_b / N_0 = 8.4$ dB, respectively.

Table 5. Comparison of the performance of the original JTIDS/Link-16 and the alternative waveforms for different values of ρ for noncoherent demodulation when $E_b / N_0 = 6$.

P_b	ρ	E_b / N_I (dB)	E_b / N_I (dB)
		Original JTIDS	Proposed Waveform
10^{-5}	1	\emptyset	11.7
10^{-5}	0.5	\emptyset	12.9
10^{-5}	0.2	\emptyset	14.1
10^{-5}	0.1	\emptyset	14.8
10^{-5}	0.05	\emptyset	14.7

From Table 5 we observe that PNI with $\rho = 0.05$ degrades the performance of the alternative waveform relative to BNI when $P_b = 10^{-5}$ and $E_b / N_0 = 6$ dB by 3.0 dB, whereas the original JTIDS/Link-16 cannot reach this probability of bit error at all.

Table 6. Comparison of the performance of the original JTIDS/Link-16 and the alternative waveforms for different values of ρ for noncoherent demodulation when $E_b / N_0 = 8.4$ dB.

P_b	ρ	E_b / N_1 (dB)	E_b / N_1 (dB)
		Original JTIDS	Proposed Waveform
10^{-5}	1	17.7	7.5
10^{-5}	0.5	18.4	9.0
10^{-5}	0.2	19.0	10.7
10^{-5}	0.1	19.6	11.0
10^{-5}	0.05	19.6	\emptyset

From Table 6, we observe that for any value of ρ the alternative waveform performs significantly better than the existing JTIDS/Link-16. We also can see that the PNI with $\rho = 0.1$ degrades the performance of the proposed system relative to BNI when $P_b = 10^{-5}$ and $E_b / N_0 = 8.4$ dB by 3.5 dB, whereas the existing JTIDS/Link-16 performance is degraded by 1.9 dB.

C. COMPARISON BETWEEN COHERENT AND NONCOHERENT DEMODULATION FOR THE ALTERNATIVE WAVEFORM

For purposes of comparison, the performance for both coherent and noncoherent demodulation of the alternative waveform when $E_b / N_0 = 8.4$ dB, for $\rho = 1$, and $\rho = 0.1$ is plotted in Figure 19.

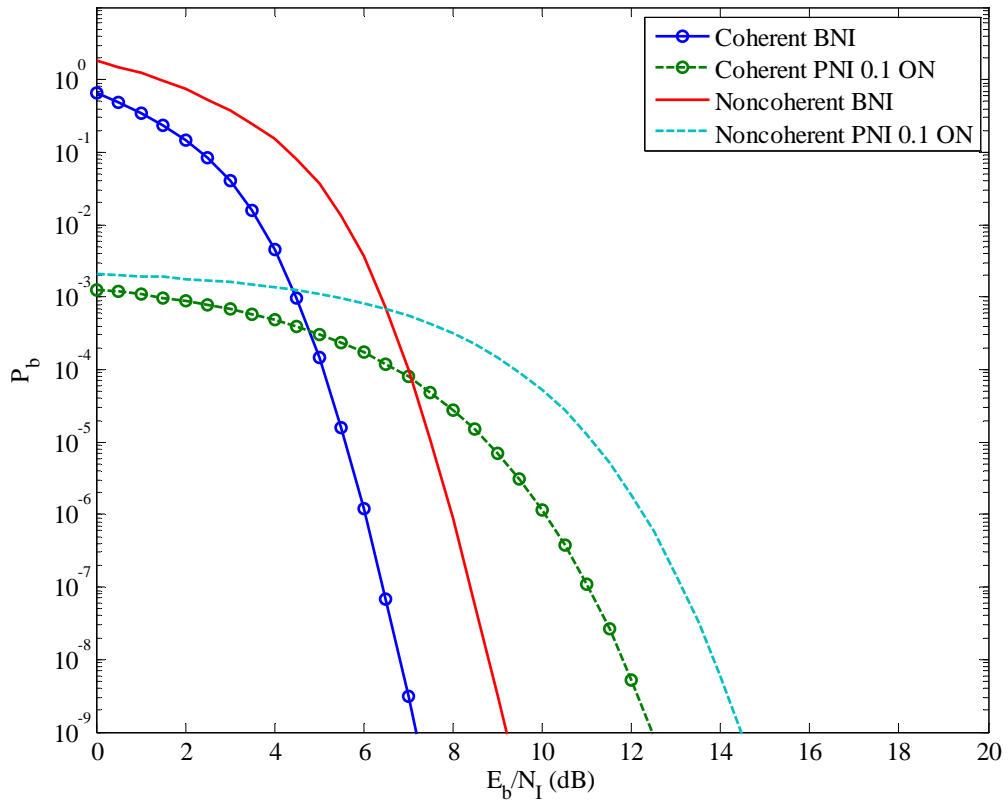


Figure 19. Comparison of the performance of the alternative waveform with both AWGN and PNI for coherent and noncoherent demodulation when $E_b / N_0 = 8.4$ dB for $\rho = 1$, and $\rho = 0.1$.

The E_b / N_1 required for $P_b = 10^{-5}$ when $E_b / N_0 = 8.4$ dB for $\rho = 1$, and $\rho = 0.1$ are listed in Table 7.

Table 7. Comparison between coherent and noncoherent demodulation of the alternative waveform in AWGN and PNI when $P_b = 10^{-5}$ and $E_b / N_0 = 8.4$ dB for $\rho = 1$, and $\rho = 0.1$.

ρ	Demodulation	P_b	E_b / N_0 (dB)
1	Coherent	10^{-5}	5.6
1	Noncoherent	10^{-5}	7.5
0.1	Coherent	10^{-5}	8.8
0.1	Noncoherent	10^{-5}	11.0

From Figure 19 and Table 7, we see that coherent demodulation performs significantly better than noncoherent. Additionally, we observe that for $E_b / N_0 = 8.4$ dB, as ρ decreases, the difference in performance between coherent and noncoherent demodulation increases from 1.9 dB for BNI to 2.2 dB for $\rho = 0.1$.

D. CHAPTER SUMMARY

In this chapter, the effects of both AWGN and PNI on the performance of the proposed waveform for both coherent and noncoherent demodulation were examined, and the results were compared to those of the original JTIDS/Link-16 waveform. In the next chapter, the performance of the alternative waveform for both coherent and noncoherent demodulation with diversity of two in an AWGN only environment is examined.

THIS PAGE INTENTIONALLY LEFT BLANK

VI. PERFORMANCE ANALYSIS OF THE ALTERNATIVE JTIDS/LINK-16 WAVEFORM FOR BOTH COHERENT AND NONCOHERENT DEMODULATION IN AWGN ONLY WITH A DIVERSITY OF TWO

In this chapter, the performance of the alternative waveform for both coherent and noncoherent demodulation with a diversity of two is examined in an AWGN only environment.

The diversity of two concept for the original JTIDS/Link-16 waveform is implied by the double-pulse structure. The data rate of the double-pulse structure is half that of the single-pulse structure. Furthermore, the average energy per bit, both channel and data, is doubled when the double-pulse structure is used. That is, JTIDS is not a constant average energy per bit system when it changes between the single and the double-pulse structure [4]. For purposes of consistency with the existing JTIDS/Link-16 waveform, in this thesis the analysis of the alternative waveform with a diversity of two is based on the average energy per bit per pulse rather than the total average energy per bit.

A. COHERENT DEMODULATION

As mentioned in Chapter II, the probability of channel symbol error for the alternative waveform for coherent demodulation in AWGN is obtained from equation (2.12) for $L=2$. Hence,

$$P_s = \frac{1}{\sqrt{2\pi}} \int_{-\infty}^{\infty} e^{\left(\frac{-u^2}{2}\right)} \left\{ 1 - \left[1 - Q\left(u + \sqrt{\frac{12.8E_b}{N_0}}\right) \right]^{31} \right\} du \quad (6.1)$$

where E_b is the average information bit energy in a pulse.

We obtain the probability of information bit error by combining equations (2.8), (2.11), (4.2), and (6.1). The performance of the alternative waveform for both no diversity and a diversity of two is shown in Figure 20.

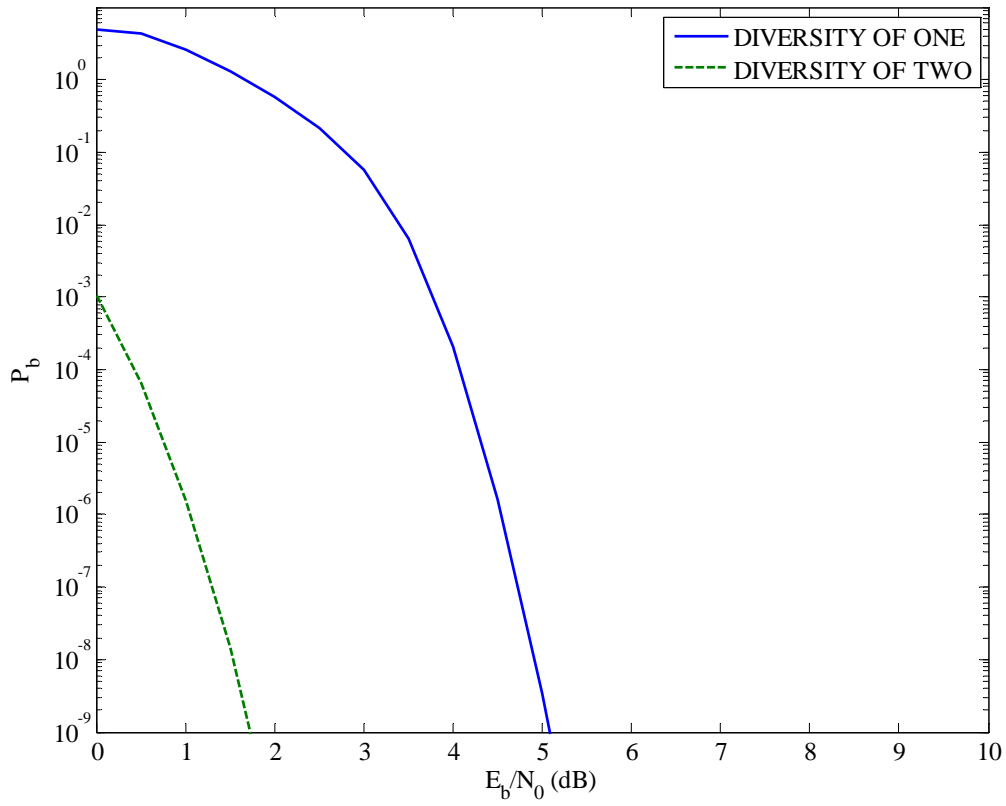


Figure 20. Performance of the alternative waveform with coherent demodulation for both no diversity and a diversity of two in AWGN.

From Table 8, we see that there is a 3.45 dB improvement for the alternative waveform with a diversity of two when $P_b = 10^{-5}$.

Table 8. Comparison of the performance of the alternative waveform for coherent demodulation in AWGN when $P_b = 10^{-5}$.

P_b	E_b / N_0 (dB)	
	No-Diversity	Diversity of Two
10^{-5}	4.2	0.75

B. NONCOHERENT DEMODULATION

As mentioned in Chapter II, the probability of channel symbol error in AWGN for noncoherent detection of M -ary orthogonal modulation with L -fold sequential diversity and soft decision combining is derived from equation (2.20). Combining equations (2.17), (2.18), and (2.20), we obtain

$$P_s = 1 - \int_0^\infty \frac{\sqrt{u_1}}{4\sigma^2 \sqrt{A_c^2}} \exp\left[\frac{-(u_1 + 4A_c^2)}{2\sigma^2}\right] I_1\left(\frac{2A_c \sqrt{u_1}}{\sigma^2}\right) \times \left[\int_0^{u_1} \frac{u_2}{4\sigma^4} \exp\left(\frac{-u_2}{2\sigma^2}\right) du_2 \right]^{M-1} du_1 \quad (6.2)$$

where $M=32$.

Equation (6.2) is analytically evaluated to obtain

$$P_s = 1 - \sum_{n=0}^{31} (-1)^n \binom{31}{n} \sum_{\mu=0}^n \binom{n}{\mu} \frac{\exp\left(\frac{2A_c^2}{(n+1)\sigma^2}\right) \exp\left(\frac{-2A_c^2}{\sigma^2}\right) \mu!}{(n+1)^{\mu+2}} \times \sum_{\rho=0}^{\mu} \frac{(-1)^\rho}{\rho!} \binom{\mu+1}{\mu-\rho} \left(\frac{-2A_c^2}{(n+1)\sigma^2}\right)^\rho \quad (6.3)$$

where $A_c^2 / \sigma^2 = E_p / N_0$ with E_p being the energy per pulse ($E_p = rmE_b$).

Combining equations (2.8), (2.11), (4.2), and (6.3), we obtain the probability of information bit error for the alternative waveform for noncoherent detection and a sequential diversity of two in AWGN. The performance of the alternative waveform for both no diversity and a diversity of two is shown in Figure 21.

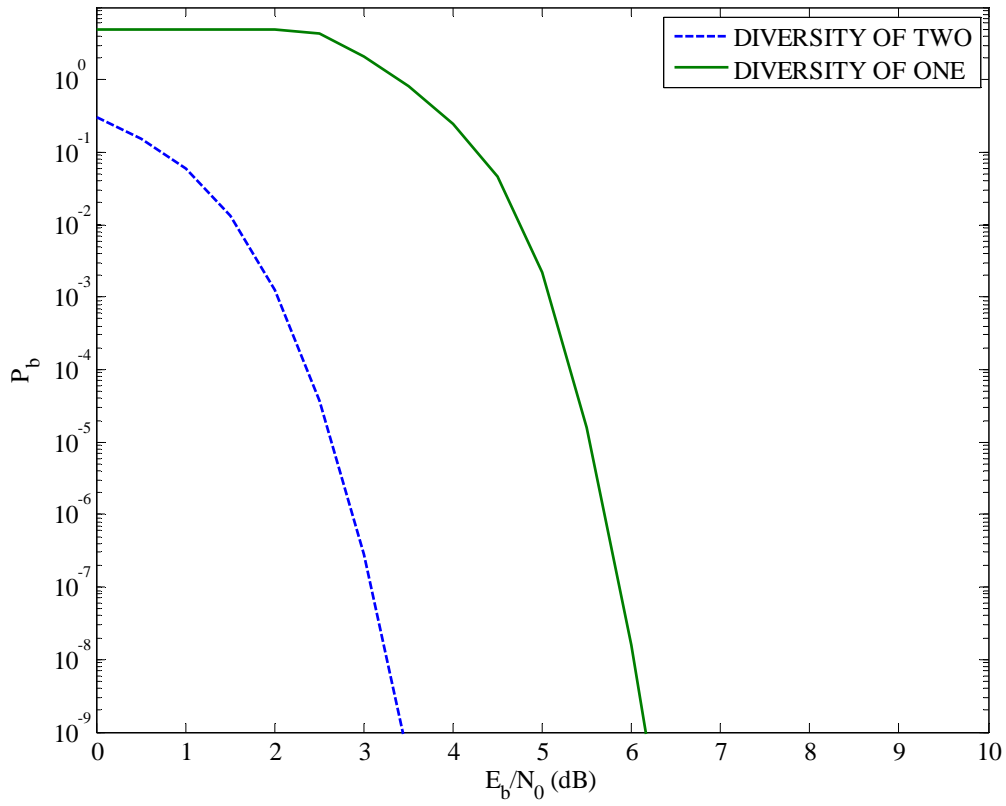


Figure 21. Performance of the alternative waveform with noncoherent demodulation for both no diversity and diversity of two in AWGN.

From Table 9, we see that there is a 2.9 dB improvement for the alternative waveform with a diversity of two when $P_b = 10^{-5}$.

Table 9. Comparison of the performance of the alternative waveform for noncoherent demodulation in AWGN when $P_b = 10^{-5}$.

P_b	E_b / N_0 (dB)	E_b / N_0 (dB)
	No-Diversity	Diversity of Two
10^{-5}	5.5	2.6

C. COMPARISON BETWEEN THE ALTERNATIVE WAVEFORM WITH A DIVERSITY OF TWO AND THE DOUBLE-PULSE STRUCTURE OF THE ORIGINAL JTIDS WAVEFORM IN AWGN

Detailed analysis of the original JTIDS/Link-16 double-pulse structure can be found in [4] and [5] and is not repeated here. The analysis made in [4] and [5] is used to obtain the performance of the original JTIDS/Link-16 waveform for both coherent and noncoherent detection in AWGN only.

The performance of both the alternative waveform with a diversity of two and the original JTIDS/Link-16 double-pulse structure are presented in Figure 22.

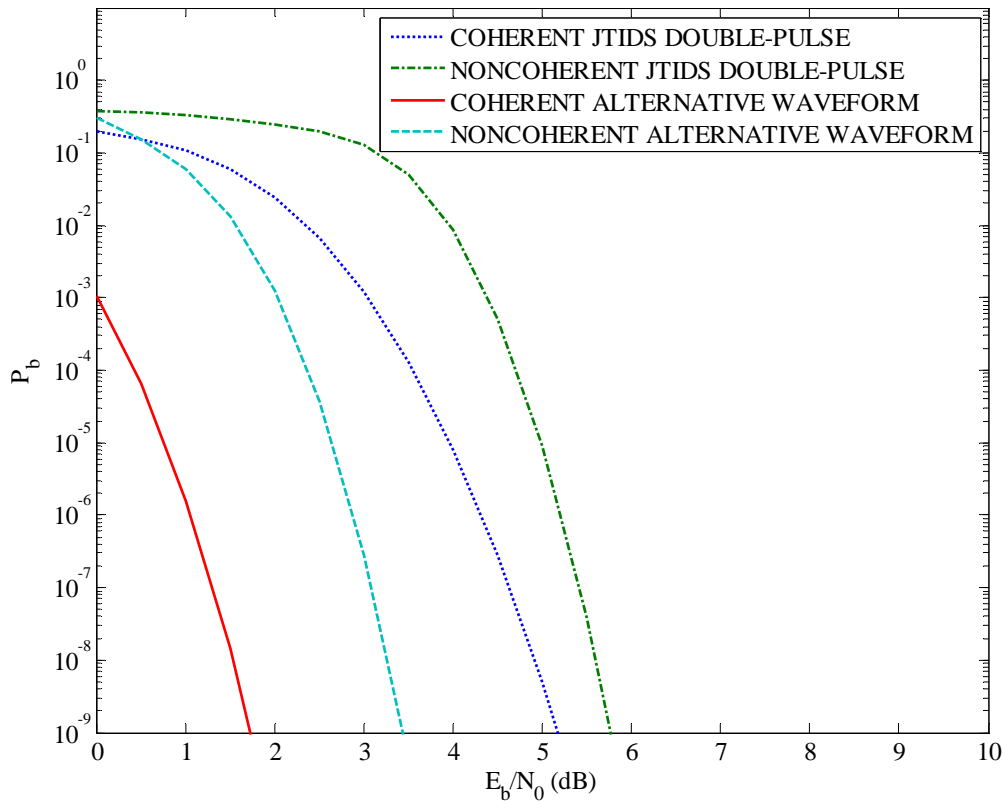


Figure 22. Performance of both the alternative waveform with a diversity of two and the existing JTIDS/Link-16 double-pulse structure for coherent and noncoherent detection in AWGN.

Table 10. Comparison between the alternative waveform with a diversity of two and the double-pulse structure of the existing JTIDS in AWGN when $P_b = 10^{-5}$.

Waveform	Demodulation	P_b	E_b / N_0 (dB)
JTIDS double-pulse	Coherent	10^{-5}	3.9
JTIDS double-pulse	Noncoherent	10^{-5}	4.9
Alternative	Coherent	10^{-5}	0.75
Alternative	Noncoherent	10^{-5}	2.6

From Figure 22 and Table 10, we observe that the proposed waveform with a diversity of two performs better than the existing JTIDS double-pulse structure for both coherent and noncoherent detection. Indeed, for $P_b = 10^{-5}$ and coherent detection, the alternative waveform has a gain of 3.15dB as compared to the JTIDS/Link-16 double-pulse structure, whereas for noncoherent detection the alternative waveform is superior to the JTIDS waveform by 2.3 dB. Additionally, from Figure 22 and Table 10, we observe that the alternative waveform performs better with coherent demodulation than with noncoherent. The difference in performance between coherent and noncoherent detection when $P_b = 10^{-5}$ is 1.85dB.

D. CHAPTER SUMMARY

In this chapter, the performance of the alternative waveform in AWGN with a diversity of two was investigated for both coherent and noncoherent detection. The performance of the proposed waveform with a diversity of two was compared to the performance of both the original JTIDS/Link-16 double-pulse structure and the alternative waveform with no diversity and proved to be superior to both. Additionally, the difference in performance between the coherent and noncoherent detection for the alternative waveform with a diversity of two was examined. In the next chapter, the performance of the alternative JTIDS/Link-16 waveform with a diversity of two in AWGN and PNI for both coherent and noncoherent detection is analyzed.

VII. PERFORMANCE ANALYSIS OF THE ALTERNATIVE JTIDS/LINK-16 WAVEFORM FOR BOTH COHERENT AND NONCOHERENT DEMODULATION IN AWGN AND PNI WITH A DIVERSITY OF TWO

In this chapter, the performance of 32-ary orthogonal signaling with concatenated coding in AWGN and PNI for both coherent and noncoherent detection with a diversity of two is considered.

A. COHERENT DEMODULATION

As mentioned in Chapter II, the probability of channel symbol error for coherent detection in AWGN and PNI with a diversity of L is obtained from equation (2.14) and is repeated here for convenience:

$$P_s = \sum_{i=0}^L \left[\binom{L}{i} \rho^i (1-\rho)^{L-i} P_s(i) \right] \quad (7.1)$$

where $P_s(i)$ is the conditional probability of channel symbol error given that i symbols experience PNI, and L is the number of the diversity receptions.

For M -ary orthogonal signaling with coherent demodulation, the output for each branch of the receiver can be represented as independent Gaussian random variables V_m where $m=1, 2, \dots, M$. The conditional probability density functions for the random variables V_m that represent the decision variables obtained by linear, soft combining of the integrator outputs given that i out of two symbols experience PNI are given by [12]

$$f_{V_1}(u_1 / 1, i) = \frac{1}{\sqrt{2\pi\sigma(i)}} \exp \left[\frac{-(u_1 - 2\sqrt{2}A_c)^2}{2\sigma^2(i)} \right] \quad (7.2)$$

for the signal branch, assumed without loss of generality to the branch one, and

$$f_{V_2}(u_2 / 1, i) = \frac{1}{\sqrt{2\pi\sigma(i)}} \exp \left[\frac{-u_2^2}{2\sigma^2(i)} \right] \quad (7.3)$$

for the non-signal branch, where

$$\sigma^2(i) = i\sigma_r^2 + (2-i)\sigma_0^2 \quad (7.4)$$

and

$$\sigma_T^2 = \sigma_I^2 + \sigma_0^2. \quad (7.5)$$

Since $\sigma_0^2 = N_0 / T_s$, and $\sigma_I^2 = N_I / T_s \rho$ from equations (7.4) and (7.5) we obtain

$$\sigma^2(i) = \frac{iN_I}{\rho T_s} + \frac{2N_0}{T_s}. \quad (7.6)$$

The conditional probability of channel symbol error given that i symbols experience PNI is obtained from [6]

$$P_s(i) = 1 - \int_{-\infty}^{\infty} f_{V_1}(u_1/1, i) \left[\int_{-\infty}^{u_1} f_{V_2}(u_2/1, i) \right]^{M-1} du_1. \quad (7.7)$$

Combining equations (7.2) through (7.7), we obtain

$$P_s(i) = \frac{1}{\sqrt{2\pi}} \int_{-\infty}^{\infty} \exp\left(\frac{-u^2}{2}\right) \left[1 - \left[1 - Q\left(u + 2\sqrt{\frac{2A_c^2}{\sigma^2(i)}}\right) \right]^{M-1} \right] du \quad (7.8)$$

which can be expressed in terms of bit energy as

$$P_s(i) = \frac{1}{\sqrt{2\pi}} \int_{-\infty}^{\infty} \exp\left(\frac{-u^2}{2}\right) \left[1 - \left[1 - Q\left(u + 2\sqrt{\frac{2rmE_b}{\frac{iN_I}{\rho} + 2N_0}}\right) \right]^{M-1} \right] du. \quad (7.9)$$

From equations (2.8), (2.11), (4.2), (7.1), and (7.9), we obtain the probability of information bit error of the alternative waveform for coherent detection with a diversity of two in AWGN and PNI. The performance for different values of ρ is shown in Figure 23 when $E_b / N_0 = 4.7$ dB. We choose E_b / N_0 to be 4.7 dB for purposes of comparison with the no-diversity structure examined in Chapter V.

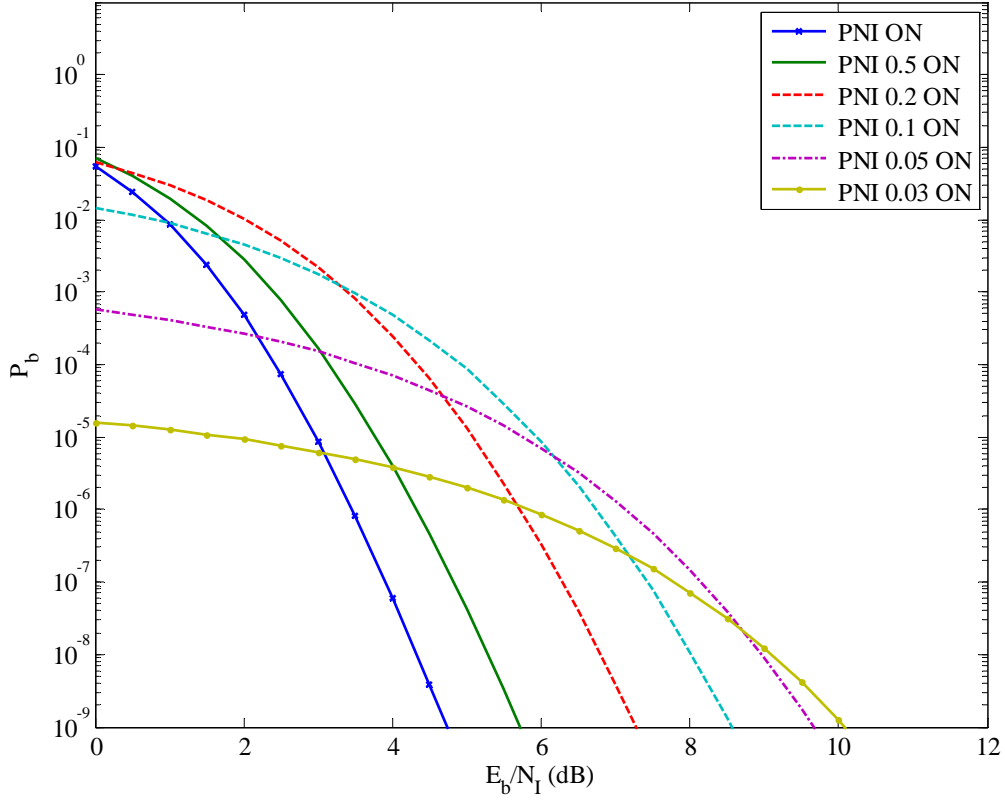


Figure 23. Performance of the alternative waveform in both AWGN and PNI for coherent demodulation with a diversity of two for $\rho = 1$, $\rho = 0.5$, $\rho = 0.2$, $\rho = 0.1$, $\rho = 0.05$, and $\rho = 0.03$ when $E_b / N_0 = 4.7$ dB.

From Figure 23, we see that PNI degrades the performance of the alternative waveform significantly. Indeed, as the fraction of time where the PNI is on is reduced, the performance of the system degrades. However, for very small values of ρ (namely $\rho \leq 0.03$), $P_b < 10^{-5}$ for all E_b / N_1 .

For purposes of comparison, the specific values of E_b / N_1 in dB when $P_b = 10^{-5}$ and $E_b / N_0 = 4.7$ dB with coherent detection in AWGN and PNI are presented in Table 11 for the alternative waveform with both no-diversity and a diversity of two, derived from Figures 13 and 23, respectively.

Table 11. Comparison of the performance of the alternative waveform with coherent demodulation in both AWGN and PNI for no diversity and a diversity of two when $P_b = 10^{-5}$.

P_b	ρ	E_b / N_I (dB)	E_b / N_I (dB)
		NO-DIVERSITY	DIVERSITY OF TWO
10^{-5}	1	10.5	3.0
10^{-5}	0.5	11.9	3.8
10^{-5}	0.2	13	5.1
10^{-5}	0.1	13.5	5.8
10^{-5}	0.05	13.6	5.8

From Table 11, we observe that for any value of ρ , the alternative waveform with a diversity of two performs much better than when there is no diversity. We also see that the PNI degrades the performance of the proposed waveform with no diversity relative to BNI when $P_b = 10^{-5}$ and $E_b / N_0 = 4.7$ dB by 3.1 dB, whereas for a diversity of two, the respective performance is degraded by 2.8 dB.

In Figure 24, we let $E_b / N_0 = 1.37$ dB. In this case we see that the performance of the alternative waveform asymptotically approaches 10^{-7} dB for $E_b / N_I \gg 1$.

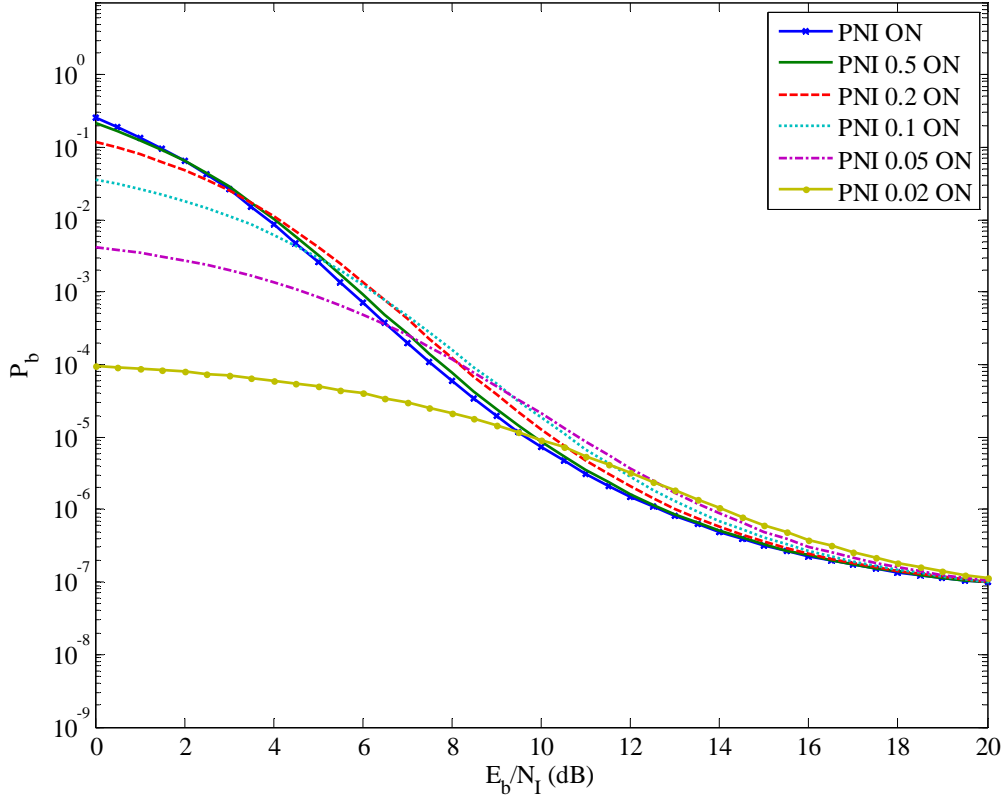


Figure 24. Performance of the alternative waveform in both AWGN and PNI environment with coherent demodulation with a diversity of two for $\rho = 1$, $\rho = 0.5$, $\rho = 0.2$, $\rho = 0.1$, $\rho = 0.05$, and $\rho = 0.02$ when $E_b / N_0 = 1.37$ dB.

From Figure 24, we see that PNI degrades the performance of the alternative waveform as the fraction of time where the PNI is on is reduced, but the degradation is much less than when E_b / N_0 is larger. When $\rho < 0.02$, the performance of the system is not affected significantly, since $P_b \leq 10^{-4}$ for all E_b / N_1 .

The values of E_b / N_1 in dB when $P_b = 10^{-5}$ and $E_b / N_0 = 1.37$ dB are presented in Table 12.

Table 12. Required E_b / N_l for $P_b = 10^{-5}$ when $E_b / N_0 = 1.37$ dB for the alternative waveform in both AWGN and PNI with coherent detection and a diversity of two .

P_b	ρ	E_b / N_l (dB) DIVERSITY OF TWO
10^{-5}	1	9.8
10^{-5}	0.5	9.9
10^{-5}	0.2	10.3
10^{-5}	0.1	10.6
10^{-5}	0.05	11
10^{-5}	0.02	9.9

In Table 12, it can be seen that the degradation in performance due to PNI as compared to BNI when $E_b / N_0 = 1.37$ dB is 1.2dB which is significantly smaller than the degradation previously obtained for $E_b / N_0 = 4.7$ dB. However, it should be noted that absolute performance is better when $E_b / N_0 = 4.7$ dB.

B. NONCOHERENT DEMODULATION

As mentioned in Chapter II, the probability of channel symbol error for the alternative waveform with noncoherent detection in AWGN and PNI with a diversity of two is obtained from equation (2.22), repeated here for convenience:

$$P_s = (1 - \rho)^2 P_s(0) + 2\rho(1 - \rho)P_s(1) + \rho^2 P_s(2). \quad (7.10)$$

Evaluating equation (2.20) for $\sigma^2 = N_0 / T_c$, we obtain $P_s(0)$ to be

$$\begin{aligned}
P_s(0) = & 1 - \sum_{n=0}^{31} (-1)^n \binom{31}{n} \sum_{\mu=0}^n \binom{n}{\mu} \frac{\exp\left(\frac{2E_p}{(n+1)N_0}\right) \exp\left(\frac{-2E_p}{N_0}\right) \mu!}{(n+1)^{\mu+2}} \\
& \times \sum_{z=0}^{\mu} \frac{(-1)^z}{z!} \binom{\mu+1}{\mu-z} \left(\frac{-2E_p}{(n+1)N_0}\right)^z
\end{aligned} \tag{7.11}$$

where E_p is the energy per pulse.

Likewise, evaluating equation (2.20) for $\sigma^2 = N_0 / T_c + N_I / \rho T_c$, we obtain $P_s(2)$ to be

$$\begin{aligned}
P_s(2) = & 1 - \sum_{n=0}^{31} (-1)^n \binom{31}{n} \sum_{\mu=0}^n \binom{n}{\mu} \frac{\exp\left(\frac{2}{(n+1)\left(\left(\frac{E_p}{N_0}\right)^{-1} + \frac{1}{\rho}\left(\frac{E_p}{N_I}\right)^{-1}\right)}\right) \exp\left(\frac{-2}{\left(\frac{E_p}{N_0}\right)^{-1} + \frac{1}{\rho}\left(\frac{E_p}{N_I}\right)^{-1}}\right) \mu!}{(n+1)^{\mu+2}} \\
& \times \sum_{z=0}^{\mu} \frac{(-1)^z}{z!} \binom{\mu+1}{\mu-z} \left(\frac{-2}{(n+1)\left(\left(\frac{E_p}{N_0}\right)^{-1} + \frac{1}{\rho}\left(\frac{E_p}{N_I}\right)^{-1}\right)}\right)^z.
\end{aligned} \tag{7.12}$$

Finally, in order to obtain $P_s(1)$ we must evaluate equation (2.26) for the pdfs $f_{V_1}(u_1/1)$ and $f_{V_2}(u_2/1)$ derived from equations (2.24) and (2.25), respectively. Because an analytic solution has not been found, a numerical evaluation is performed. Our objective is to express equation (2.26) in terms of only one parameter (namely E_p / N_I). Hence, starting with equation (2.24) and substituting $y \times \sigma^2$ for α , we obtain

$$f_{v_1}(u_1/1) = \int_0^{u_1/\sigma_0^2} \frac{1}{4\sigma_0^2} \exp\left(\frac{-y}{2} - \frac{E_p}{N_0}\right) I_0\left(\sqrt{2y} \frac{E_p}{N_0}\right) \frac{1}{\left(1 + \frac{\sigma_l^2}{\sigma_0^2}\right)} \quad (7.13)$$

$$\times \exp\left[\frac{y}{2\left(1 + \frac{\sigma_l^2}{\sigma_0^2}\right)} - \frac{u_1}{2\sigma_0^2\left(1 + \frac{\sigma_l^2}{\sigma_0^2}\right)} - \frac{E_p}{N_0\left(1 + \frac{\sigma_l^2}{\sigma_0^2}\right)}\right] I_0\left[\sqrt{\frac{E_p}{N_0}} \frac{1}{\left(1 + \frac{\sigma_l^2}{\sigma_0^2}\right)} \sqrt{\frac{2u_1}{\sigma_0^2} - 2y}\right] dy.$$

Next, combining equations (2.25), (2.26), and (7.13) and substituting $x \times \sigma_0^2$ for u_1 , we obtain

$$\begin{aligned} P_s &= 1 - \int_0^\infty \int_0^x \frac{1}{4} \exp\left(\frac{-y}{2} - \frac{E_p}{N_0}\right) I_0\left(\sqrt{2y} \frac{E_p}{N_0}\right) \\ &\times \exp\left[\frac{y}{2\left(1 + \frac{\sigma_l^2}{\sigma_0^2}\right)} - \frac{x}{2\left(1 + \frac{\sigma_l^2}{\sigma_0^2}\right)} - \frac{E_p}{N_0\left(1 + \frac{\sigma_l^2}{\sigma_0^2}\right)}\right] \\ &\times \frac{1}{\left(1 + \frac{\sigma_l^2}{\sigma_0^2}\right)} I_0\left[\sqrt{\frac{E_p}{N_0}} \frac{1}{\left(1 + \frac{\sigma_l^2}{\sigma_0^2}\right)} \sqrt{2x - 2y}\right] \\ &\times \left\{ -\frac{\sigma_0^2}{\sigma_l^2} \left[\left(1 - e^{-\frac{x}{2}}\right) - \left(1 + \frac{\sigma_l^2}{\sigma_0^2}\right) \left(1 - e^{-\frac{x}{2\left(1 + \frac{\sigma_l^2}{\sigma_0^2}\right)}}\right) \right] \right\}^{M-1} dy dx \end{aligned} \quad (7.14)$$

where σ_l^2 / σ_0^2 can be expressed as

$$\frac{\sigma_l^2}{\sigma_0^2} = \frac{\left(\frac{E_p}{N_l}\right)^{-1}}{\rho \left(\frac{E_p}{N_0}\right)}. \quad (7.15)$$

Consequently, equation (7.14) can be evaluated numerically for specific values of E_p / N_0 and E_b / N_1 .

Combining equations (2.8), (2.11), (2.25), (4.2), (7.14), and (7.10), we obtain the probability of information bit error of the alternative waveform with noncoherent detection in an AWGN plus PNI environment with a diversity of two. The performance for different values of ρ is presented in Figure 25 when $E_b / N_0 = 6$ dB. E_b / N_0 is chosen to be 6 dB for purposes of comparison with the no-diversity structure examined in Chapter V.

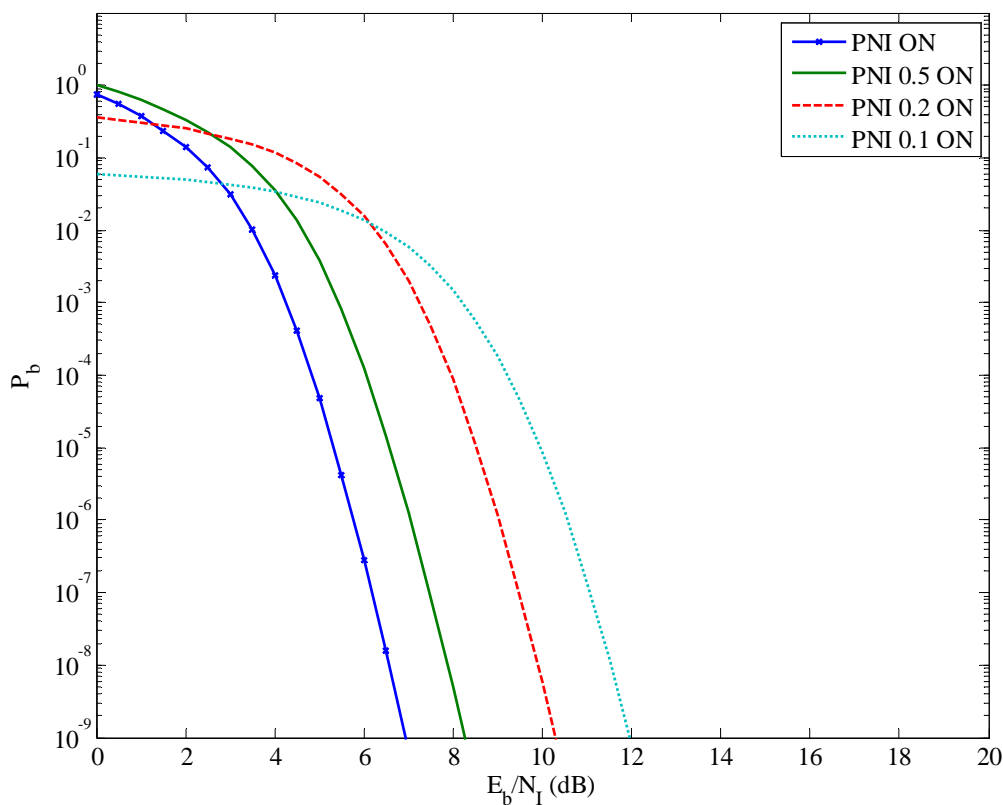


Figure 25. Performance of the alternative waveform in both AWGN and PNI with noncoherent demodulation with a diversity of two for $\rho = 1$, $\rho = 0.5$, $\rho = 0.2$, and $\rho = 0.1$ when $E_b / N_0 = 6$ dB.

From Figure 25, we observe that PNI degrades the performance of the alternative waveform significantly. Again as the fraction of time where the PNI is on is reduced, the performance of the system degrades.

For purposes of comparison, the specific E_b / N_I in dB when $P_b = 10^{-5}$ and $E_b / N_0 = 6$ dB are presented in Table 13 for the alternative waveform with both no diversity and with a diversity of two for noncoherent detection in AWGN and PNI as derived from Figures 15 and 25, respectively.

Table 13. Comparison of the performance of the alternative waveform with noncoherent demodulation in both AWGN and PNI for no diversity and a diversity of two for $P_b = 10^{-5}$ [From author].

P_b	ρ	E_b / N_I (dB)	E_b / N_I (dB)
		NO-DIVERSITY	DIVERSITY OF TWO
10^{-5}	1	11.7	5.3
10^{-5}	0.5	12.9	6.5
10^{-5}	0.2	14.1	8.5
10^{-5}	0.1	14.8	10

From Table 13, we observe that for any value of ρ the alternative waveform with a diversity of two performs much better than with no diversity. We also see that the PNI degrades the performance of the proposed waveform with no diversity relative to BNI when $P_b = 10^{-5}$ and $E_b / N_0 = 6$ dB by 3.1 dB, whereas for a diversity of two the respective performance is degraded by 4.7 dB.

In Figure 26, $E_b / N_0 = 3.11$ dB. In this case, the performance of the alternative waveform with a diversity of two asymptotically approaches 10^{-7} dB for $E_b / N_I \gg 1$.

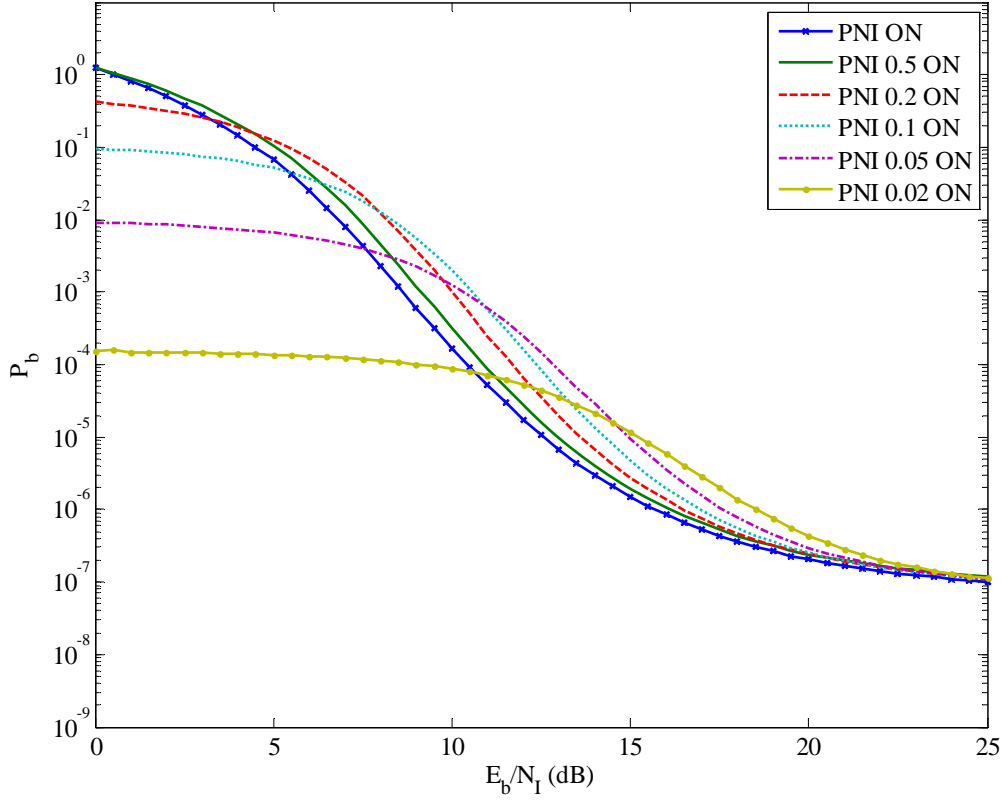


Figure 26. Performance of the alternative waveform in both AWGN and PNI with noncoherent demodulation and a diversity of two for $\rho = 1$, $\rho = 0.5$, $\rho = 0.2$, $\rho = 0.1$, $\rho = 0.05$, and $\rho = 0.02$ when $E_b / N_0 = 3.11$ dB.

From Figure 26, we see that PNI degrades the performance of the alternative waveform as the fraction of time when the PNI is on is reduced. When $\rho \leq 0.02$, the performance of the system is not affected much since $P_b < 10^{-4}$ for all E_b / N_1 .

The values of E_b / N_1 in dB when $P_b = 10^{-5}$ and $E_b / N_0 = 3.11$ dB are presented in Table 14.

Table 14. Required E_b / N_l for $P_b = 10^{-5}$ when $E_b / N_0 = 3.11$ dB for the alternative waveform in both AWGN and PNI with noncoherent detection and a diversity of two.

P_b	ρ	E_b / N_l (dB) DIVERSITY OF TWO
10^{-5}	1	12.6
10^{-5}	0.5	13.0
10^{-5}	0.2	13.7
10^{-5}	0.1	14.4
10^{-5}	0.05	15.0
10^{-5}	0.02	15.2

In Table 14, we see that the degradation in performance due to PNI as compared to BNI when $E_b / N_0 = 3.11$ dB is 2.6 dB, which is significantly smaller than the degradation previously obtained for $E_b / N_0 = 6$ dB. Again, however, absolute performance is much better when $E_b / N_0 = 6$ dB regardless ρ .

C. COMPARISON BETWEEN COHERENT AND NONCOHERENT DEMODULATION FOR THE ALTERNATIVE WAVEFORM

For purposes of comparison, the performance for both coherent and noncoherent demodulation of the alternative waveform when $E_b / N_0 = 3.11$ dB for $\rho = 1$, and $\rho = 0.05$ is plotted in Figure 27.

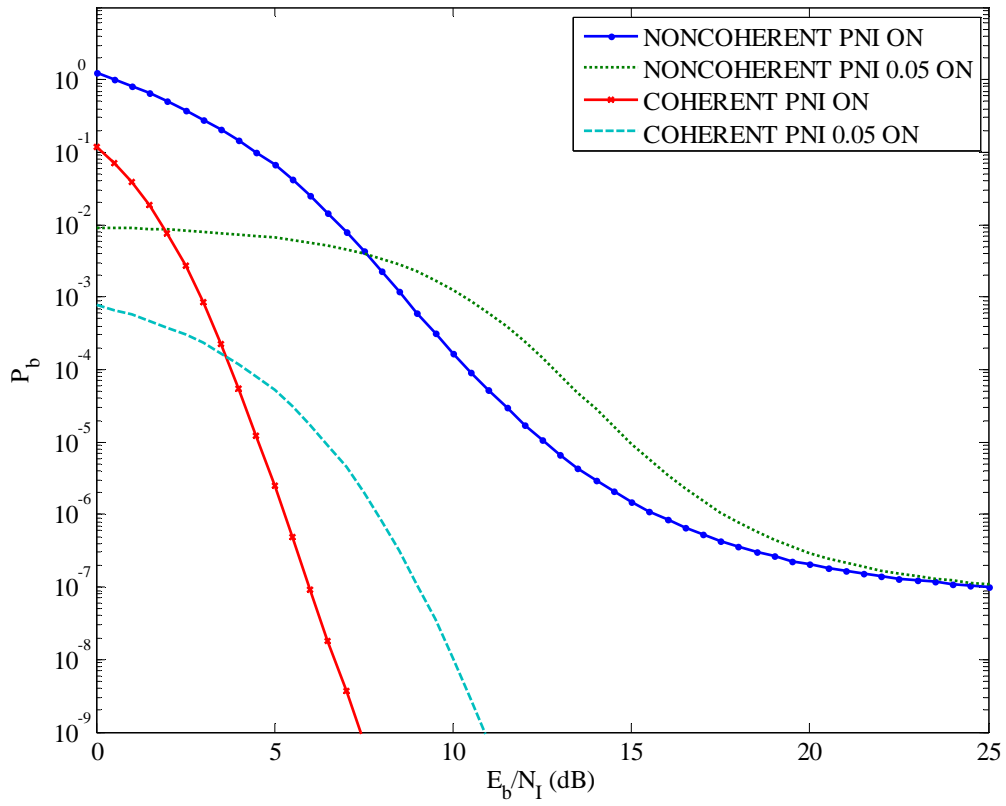


Figure 27. Comparison of the performance of the alternative waveform with a diversity of two for coherent and noncoherent detection in AWGN and PNI for $\rho = 1$ and $\rho = 0.05$ when $E_b / N_0 = 3.11$ dB.

The E_b / N_1 in dB required for $P_b = 10^{-5}$ when $E_b / N_0 = 3.11$ dB for $\rho = 1$ and $\rho = 0.05$ are listed in Table 15.

Table 15. Comparison between coherent and noncoherent demodulation for the alternative waveform in an AWGN plus PNI environment with a diversity of two when $P_b = 10^{-5}$ and $E_b / N_0 = 3.11$ dB for $\rho = 1$ and $\rho = 0.05$.

ρ	Demodulation	P_b	E_b / N_t (dB)
1	Coherent	10^{-5}	4.5
1	Noncoherent	10^{-5}	12.6
0.05	Coherent	10^{-5}	6.5
0.05	Noncoherent	10^{-5}	15.0

From Figure 27 and Table 15, we observe that coherent demodulation performs significantly better than noncoherent. Additionally, we observe that for $E_b / N_0 = 3.11$ dB, as ρ decreases, the difference in performance between coherent and noncoherent demodulation increases from 8.1 dB for BNI to 8.5 dB for $\rho = 0.05$.

D. COMPARISON BETWEEN THE ALTERNATIVE WAVEFORM WITH A DIVERSITY OF TWO AND THE ORIGINAL JTIDS/LINK-16 DOUBLE-PULSE STRUCTURE WITH COHERENT DETECTION IN AWGN AND PNI

The probability of information bit error for both the alternative waveform with a diversity of two and the original JTIDS/Link-16 double-pulse structure with coherent demodulation in AWGN and PNI for different values of ρ when $E_b / N_0 = 7.78$ dB is shown in Figure 28. Detailed analysis of the original JTIDS/Link-16 double-pulse structure performance can be found in [5] and is not repeated here.

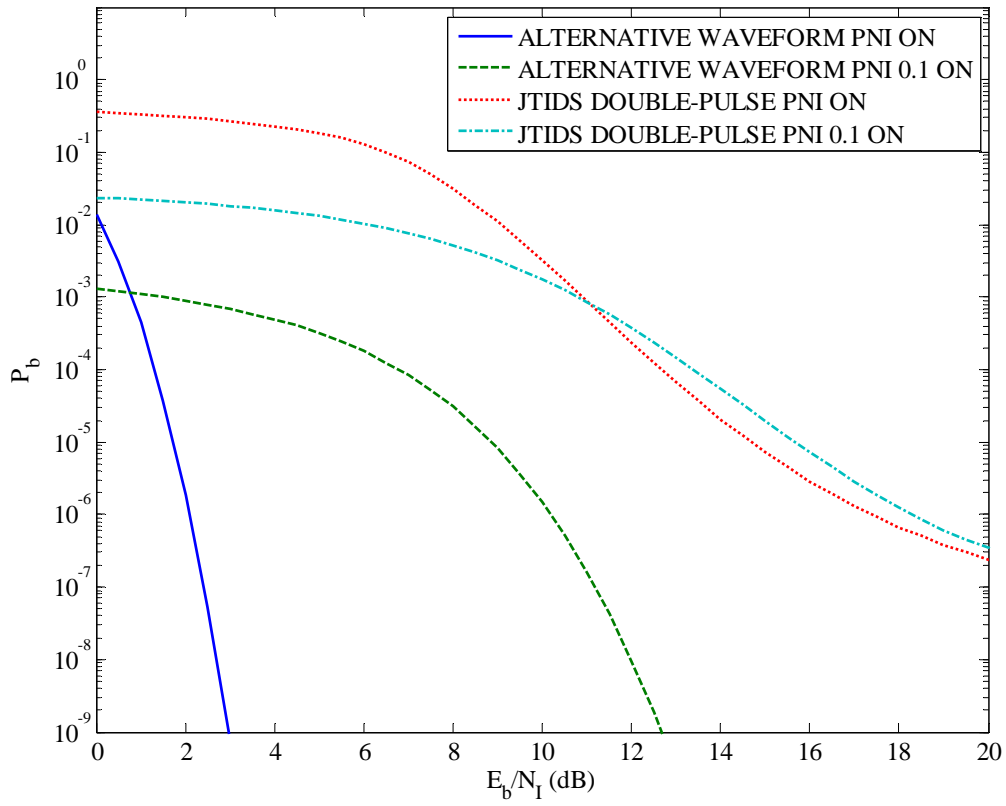


Figure 28. Performance of the alternative waveform with a diversity of two and the original JTIDS/Link-16 double-pulse structure with coherent demodulation in AWGN and PNI when $E_b / N_0 = 7.78$ dB for $\rho = 1$ and $\rho = 0.1$.

The E_b / N_1 in dB required for $P_b = 10^{-5}$ when $E_b / N_0 = 7.78$ dB for $\rho = 1$ and $\rho = 0.1$ are listed in Table 16.

Table 16. Comparison between the alternative waveform with a diversity of two and the double-pulse structure of the existing JTIDS in AWGN and PNI when $E_b / N_0 = 7.78$ dB and $P_b = 10^{-5}$.

Waveform	ρ	P_b	E_b / N_t (dB)
JTIDS double-pulse	1	10^{-5}	14.7
JTIDS double-pulse	0.1	10^{-5}	15.7
Alternative	1	10^{-5}	1.7
Alternative	0.1	10^{-5}	8.8

From Figure 28 and Table 16, we observe that the proposed waveform performs significantly better than the original JTIDS/Link-16 double pulse structure. Indeed, when $P_b = 10^{-5}$, $E_b / N_0 = 7.78$ dB and $\rho = 1$, the alternative waveform has a gain of 13 dB compared to the JTIDS/Link-16 double-pulse structure, whereas for $\rho = 0.1$ the gain is 6.9 dB.

Comparison of the proposed waveform with a diversity of two and the JTIDS/Link-16 double-pulse structure in an AWGN plus PNI environment with noncoherent detection is not considered in this thesis. However, we speculate that the proposed waveform would perform better since this is the case for all other scenarios that have been considered.

E. CHAPTER SUMMARY

In this chapter, the performance of the alternative waveform with a diversity of two was investigated for both coherent and noncoherent detection in AWGN and PNI. The difference in performance between coherent and noncoherent detection was examined. The performance of the proposed waveform with a diversity of two and with no diversity were compared, and the diversity of two structure proved to be superior to the structure with no diversity. Additionally, a comparison between the proposed waveform with a diversity of two and the existing JTIDS/Link-16 double-pulse structure

for coherent demodulation was made. In the next chapter the performance of the alternative JTIDS/Link-16 waveform in AWGN and PNI for both coherent and noncoherent detection with a diversity of two and perfect side information (PSI) is analyzed.

THIS PAGE INTENTIONALLY LEFT BLANK

VIII. PERFORMANCE ANALYSIS OF THE ALTERNATIVE JTIDS/LINK-16 WAVEFORM FOR BOTH COHERENT AND NONCOHERENT DEMODULATION IN AWGN AND PNI WITH A DIVERSITY OF TWO AND PSI

In this chapter, the performance of the alternative waveform in an AWGN plus PNI environment for both coherent and noncoherent demodulation with a diversity of two and PSI is considered.

In some cases, the system performance can be improved further if we have some information regarding which pulse is jammed and which is not. When available, this information is called side information. Perfect side information is not realistic but gives a benchmark against which to measure receivers which have imperfect or no side information. For PSI, we assume that the jammed pulse is disregarded except when all pulses are jammed. Given this assumption, PSI has no effect on a no-diversity structure but will affect a structure with a diversity of two [5].

A. COHERENT DEMODULATION

In Chapter VII we saw that the probability of channel symbol error in AWGN and PNI with a diversity of two is obtained from equation (7.1), which for the case of $L=2$ reduces to

$$P_s = (1 - \rho)^2 P_s(0) + 2\rho(1 - \rho)P_s(1) + \rho^2 P_s(2). \quad (8.1)$$

In the case of coherent detection and PSI, $P_s(0)$ is the conditional probability of channel symbol error when PNI does not affect either diversity reception and, thus, can be expressed by equation (2.12), repeated here for convenience:

$$P_s(0) = \frac{1}{\sqrt{2\pi}} \int_{-\infty}^{\infty} e^{\left(\frac{-u^2}{2}\right)} \left\{ 1 - \left[1 - Q\left(u + 2\sqrt{\frac{rmE_b}{N_0}}\right) \right]^{31} \right\} du. \quad (8.2)$$

When both pulses are affected by PNI, discarding the affected pulses is unacceptable since the whole signal would be discarded. Hence, the conditional probability of channel symbol error in this case is obtained from equation (7.9) for $i=2$ and is repeated here for convenience:

$$P_s(2) = \frac{1}{\sqrt{2\pi}} \int_{-\infty}^{\infty} \exp\left(\frac{-u^2}{2}\right) \left[1 - \left[1 - Q\left(u + 2\sqrt{\frac{2rmE_b}{iN_I + 2N_0}}\right) \right]^{31} \right] du. \quad (8.3)$$

Finally, when one out of two pulses is affected by PNI the decision at the output of the demodulator is made based only on the unjammed pulse (the affected pulse is discarded). Consequently, the conditional probability of channel symbol error when only one of the two diversity receptions suffers PNI is obtained from equation (2.2) and is repeated here for convenience:

$$P_s(1) = \frac{1}{\sqrt{2\pi}} \int_{-\infty}^{\infty} e^{\left(\frac{-u^2}{2}\right)} \left\{ 1 - \left[1 - Q\left(u + \sqrt{\frac{2rmE_b}{N_0}}\right) \right]^{31} \right\} du. \quad (8.4)$$

Combining equations (2.8), (2.11), (4.2), and (8.1) through (8.4), we obtain the probability of information bit error of the alternative waveform with a diversity of two, for coherent detection in AWGN and PNI with PSI. The performance for different values of ρ is presented in Figures 29 and 30 for $E_b/N_0 = 4.7$ dB and $E_b/N_0 = 1.37$ dB, respectively. These values of E_b/N_0 were chosen for purposes of comparison with the respective no-side information structure discussed in Chapter VII.

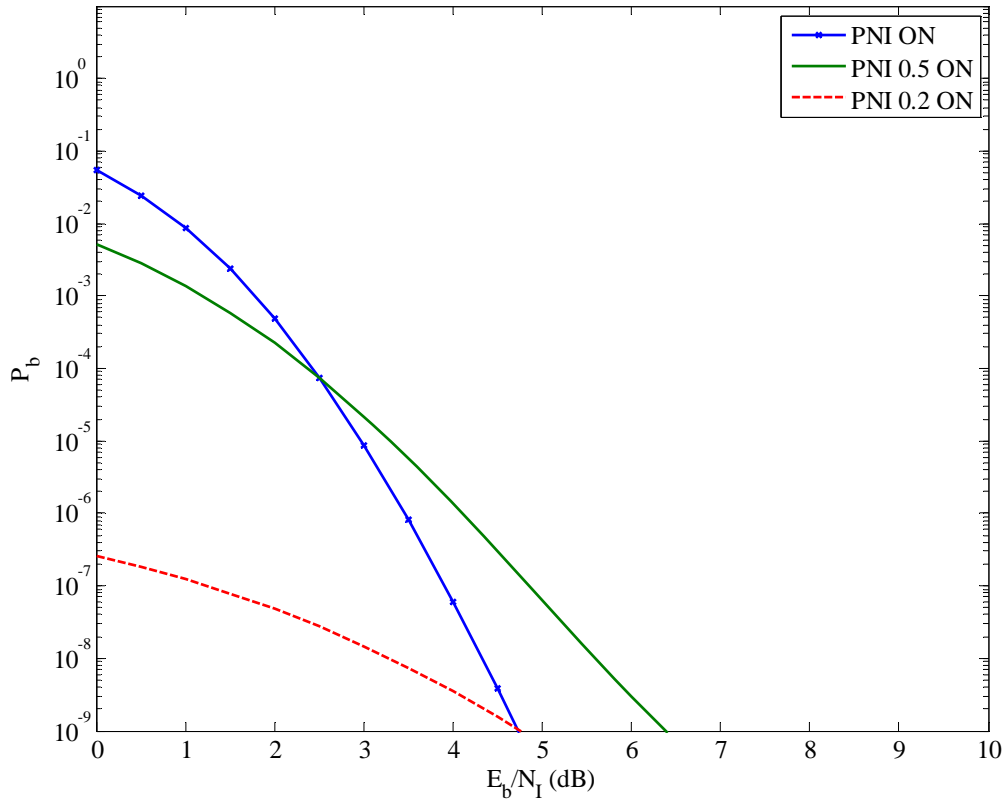


Figure 29. Performance of the alternative waveform with a diversity of two for coherent detection in AWGN and PNI with PSI when $E_b / N_0 = 4.7$ dB for $\rho = 1$, $\rho = 0.5$, and $\rho = 0.2$.

Table 17. Comparison between the diversity of two structure of the alternative waveform in AWGN and PNI with coherent demodulation and no-side information and the same structure with PSI when $E_b / N_0 = 4.7$ dB.

P_b	ρ	E_b / N_I (dB)	E_b / N_I (dB)
		NO-SIDE INFORMATION	WITH PERFECT SIDE INFORMATION
10^{-5}	1	3.0	3.0
10^{-5}	0.5	3.8	3.3
10^{-5}	0.2	5.1	\emptyset
10^{-5}	0.1	5.8	\emptyset
10^{-5}	0.05	5.8	\emptyset

From Figure 29, Figure 23, and Table 17, we observe that when $E_b / N_0 = 4.7$ dB and $\rho = 1$ there is no difference in performance whether PSI is used or not. This is a consequence of the fact that $\rho = 1$ implies that the channel is experiencing barrage jamming which means that all pulses are jammed and thus none are discarded when PSI is used. When $P_b = 10^{-5}$ and $\rho = 0.5$, the PSI structure performs 0.5dB better than the no side information structure. Finally, when $\rho \leq 0.2$, the alternative waveform with PSI has $P_b < 10^{-5}$ for all E_b / N_I .

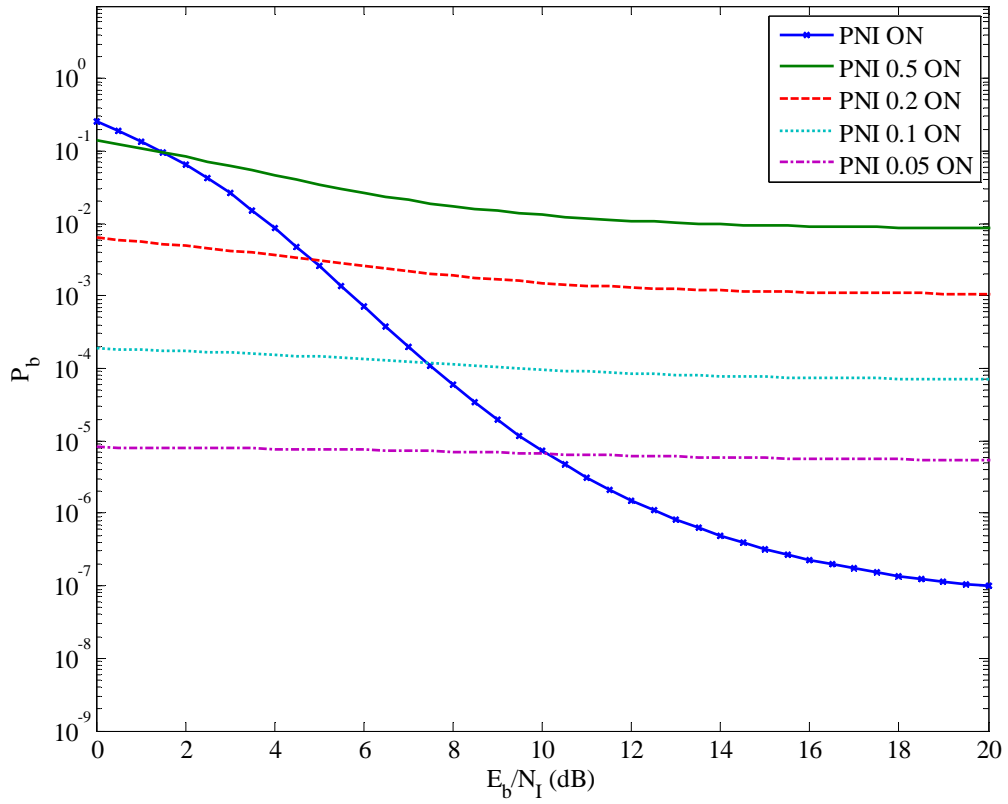


Figure 30. Performance of the alternative waveform with a diversity of two for coherent detection in AWGN and PNI with PSI when $E_b / N_0 = 1.37$ dB for $\rho = 1, \rho = 0.5, \rho = 0.2, \rho = 0.1$, and $\rho = 0.05$.

Table 18. Comparison between the diversity of two structure of the alternative waveform in AWGN and PNI with coherent demodulation and no-side information and the same structure with PSI when $E_b / N_0 = 1.37$ dB.

P_b	ρ	E_b / N_I (dB)	E_b / N_I (dB)
		NO-SIDE INFORMATION	WITH PERFECT SIDE INFORMATION
10^{-5}	1	9.8	9.8
10^{-5}	0.5	9.9	\emptyset
10^{-5}	0.2	10.3	\emptyset
10^{-5}	0.1	10.6	\emptyset
10^{-5}	0.05	11	\emptyset

From Figure 30, Figure 24, and Table 18, we observe that when $E_b / N_0 = 1.37$ dB and $\rho = 1$, there is no difference in performance whether PSI is used or not. However, we see that for $0.05 < \rho < 1$, the performance with PSI is worse as compared to that without PSI. Indeed as E_b / N_I gets larger, the probability of information bit error goes asymptotically to numerical values above 10^{-5} . This is because the E_b / N_0 is very low and, hence, the AWGN results in a significantly high probability of error. On the other hand, when E_b / N_I is large, the affected pulse is weakly jammed, so discarding a weakly jammed pulse in a channel where E_b / N_0 is very low degrades further the performance of the system. Finally, for $\rho \leq 0.05$ with PSI, $P_b \leq 10^{-5}$ even for very small values of E_b / N_I .

B. NONCOHERENT DEMODULATION

As we have already mentioned, equation (8.1) holds in determining the probability of channel symbol error for the alternative waveform in AWGN and PNI with a diversity of two for noncoherent demodulation as well as for coherent demodulation.

Additionally, the concept of perfect side information works in the same way for both types of demodulation. However, the conditional probabilities of channel symbol error for coherent and noncoherent detection are obtained differently.

In the case of noncoherent detection and PSI, $P_s(0)$ is obtained from equation (7.11), and $P_s(2)$ is obtained from equation (7.12). The conditional probability of channel symbol error when only one of the two diversity receptions suffers PNI is obtained from equation (2.4).

Combining equations (2.8), (2.11), (2.4), (4.2), (7.11), (7.12), and (8.1), we obtain the probability of information bit error of the alternative waveform with a diversity of two for noncoherent detection in AWGN and PNI with PSI. The performances for different values of ρ are presented in Figures 30 and 31 for $E_b / N_0 = 6$ dB and $E_b / N_0 = 3.11$ dB, respectively. These specific values of E_b / N_0 were chosen for purposes of comparison with the respective no-side information structure of Chapter VII.

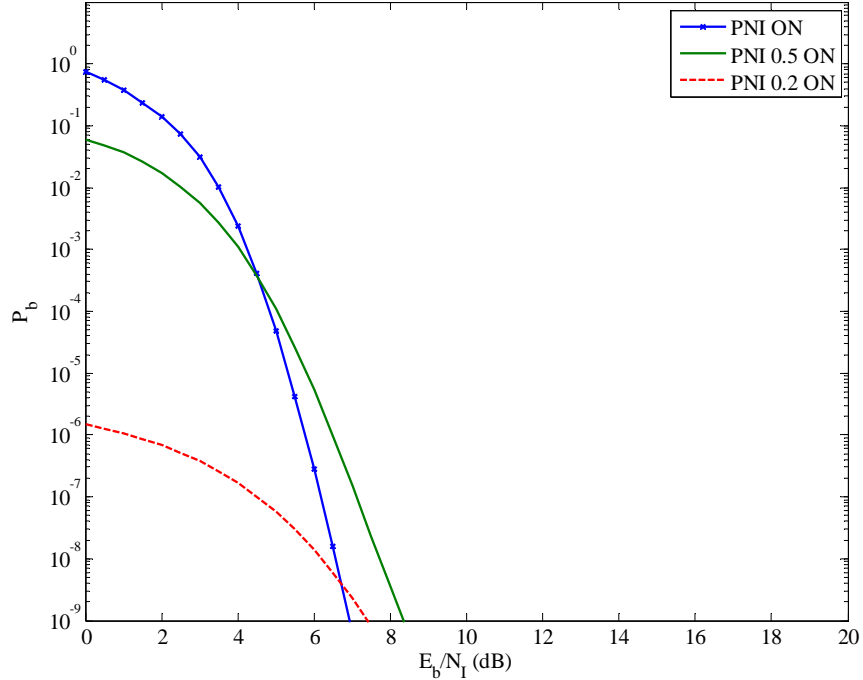


Figure 31. Performance for noncoherent detection in AWGN and PNI with PSI when $E_b / N_0 = 6$ dB for $\rho = 1$, $\rho = 0.5$, and $\rho = 0.2$.

Table 19. Comparison between the diversity of two structure of the alternative waveform in AWGN and PNI with noncoherent demodulation and no-side information and the same structure with PSI when $E_b / N_0 = 6$ dB.

P_b	ρ	E_b / N_I (dB)	E_b / N_I (dB)
		NO-SIDE INFORMATION	WITH PERFECT SIDE INFORMATION
10^{-5}	1	5.3	5.3
10^{-5}	0.5	6.5	5.8
10^{-5}	0.2	8.5	\emptyset
10^{-5}	0.1	10	\emptyset

From Figure 31, Figure 25, and Table 19, we observe again that, when $E_b / N_0 = 6$ dB and $\rho = 1$, there is no difference in performance whether PSI is used or not. This is a consequence of the fact that $\rho = 1$ implies that the channel is experiencing barrage jamming which means that all pulses are jammed and thus none are discarded when PSI is used. When $P_b = 10^{-5}$ and $\rho = 0.5$, the PSI structure performs 0.7dB better than the no side information structure. Additionally, when $\rho \leq 0.2$, the alternative waveform with PSI has $P_b < 10^{-5}$ for all E_b / N_I .

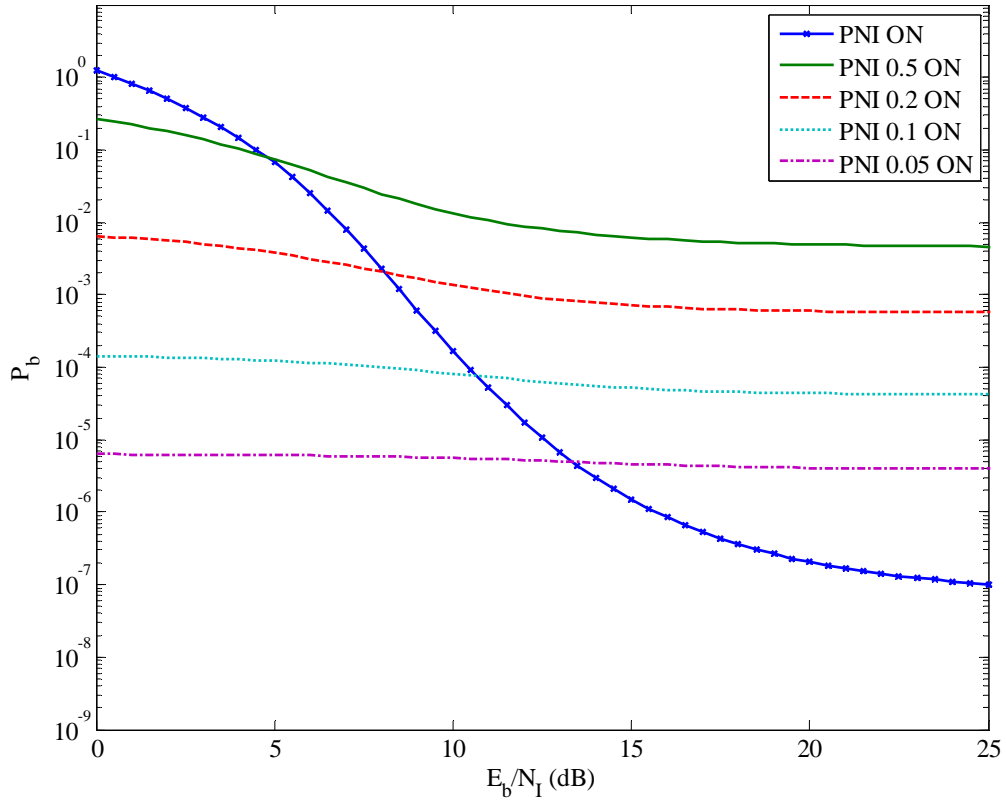


Figure 32. Performance of the alternative waveform with a diversity of two for noncoherent detection in AWGN and PNI with PSI when $E_b / N_0 = 3.11$ dB for $\rho = 1, \rho = 0.5, \rho = 0.2, \rho = 0.1$, and $\rho = 0.05$.

Table 20. Comparison between the diversity of two structure of the alternative waveform in AWGN and PNI with noncoherent demodulation and no-side information and the same structure with PSI when $E_b / N_0 = 3.11$ dB.

P_b	ρ	E_b / N_I (dB)	E_b / N_I (dB)
		NO-SIDE INFORMATION	WITH PERFECT SIDE INFORMATION
10^{-5}	1	12.6	12.6
10^{-5}	0.5	13.0	\emptyset
10^{-5}	0.2	13.7	\emptyset
10^{-5}	0.1	14.4	\emptyset
10^{-5}	0.05	15.0	\emptyset

From Figure 32, Figure 26, and Table 20, we observe again that when $E_b / N_0 = 3.11$ dB and $\rho = 1$ there is no difference in performance whether PSI is used or not. However, we see that for $0.05 < \rho < 1$, the performance with PSI is worse as compared to that without PSI. Indeed, as E_b / N_I gets larger the probability of information bit error asymptotically approaches numerical values greater than 10^{-5} . As previously stated, this is, first, because E_b / N_0 is very low and, hence, the AWGN results in a significantly higher probability of error and, second, because when E_b / N_I is large the affected pulse is weakly jammed, so discarding a weakly jammed pulse in a channel where E_b / N_0 is very low degrades further the performance of the system. Finally, in this case too $\rho \leq 0.05$ results in $P_b \leq 10^{-5}$ even for very small values of E_b / N_I .

C. COMPARISON BETWEEN COHERENT AND NONCOHERENT DEMODULATION

For purposes of comparison, the performance for both coherent and noncoherent demodulation of the alternative waveform with PSI when $E_b / N_0 = 6$ dB for $\rho = 1$ and $\rho = 0.05$ is plotted in Figure 33.

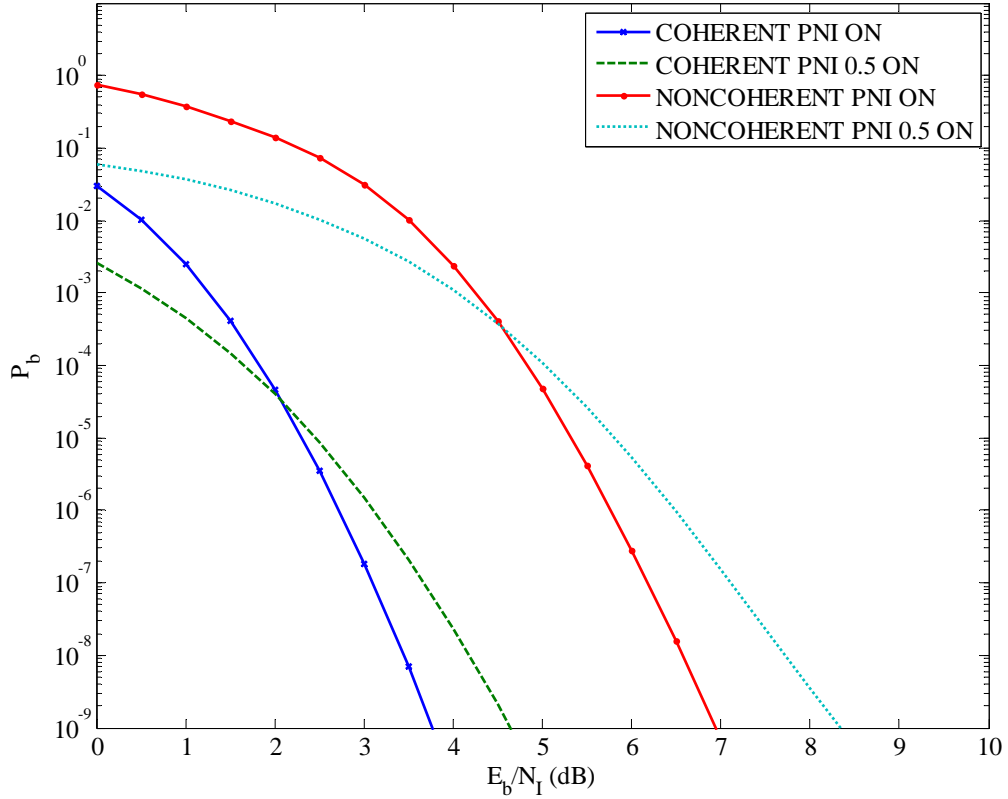


Figure 33. Comparison of the performance of the alternative waveform with a diversity of two and PSI between coherent and noncoherent detection in AWGN and PNI for $\rho = 1$ and $\rho = 0.5$ when $E_b / N_0 = 6$ dB.

The E_b / N_1 in dB required for $P_b = 10^{-5}$ when $E_b / N_0 = 6$ dB for $\rho = 1$ and $\rho = 0.5$ are listed in Table 21.

Table 21. Comparison between coherent and noncoherent demodulation for the alternative waveform in AWGN and PNI with a diversity of two and PSI when $P_b = 10^{-5}$ and $E_b / N_0 = 6$ dB for $\rho = 1$ and $\rho = 0.5$.

ρ	Demodulation	P_b	E_b / N_t (dB)
1	Coherent	10^{-5}	2.3
1	Noncoherent	10^{-5}	5.3
0.5	Coherent	10^{-5}	2.5
0.5	Noncoherent	10^{-5}	5.8

From Figure 33 and Table 21, we observe that coherent demodulation performs better than noncoherent. Indeed, there is a 3.0 dB difference when $\rho = 1$ and a 3.3 dB difference when $\rho = 0.5$.

D. CHAPTER SUMMARY

In this chapter, the performance of the alternative waveform with a diversity of two and PSI was investigated for both coherent and noncoherent detection in AWGN and PNI. Additionally, the difference in performance between coherent and noncoherent detection was examined. In the next chapter, the findings of this thesis are summarized.

IX. CONCLUSIONS AND FUTURE WORK

An alternative JTIDS/Link-16 waveform, 32-ary orthogonal signaling with a concatenated code consisting of a (31, 25) RS inner code and a 4/5 convolutional outer code, was presented in this thesis. The performance of the proposed waveform with no diversity as well as with a diversity of two was analyzed for both AWGN only as well as AWGN plus PNI for both coherent and noncoherent demodulation. The effect of perfect-side information was also investigated.

Based on the results obtained, the proposed waveform was found to perform better than the original JTIDS/Link-16 waveform. When only AWGN is present, the alternative waveform with no diversity outperforms the JTIDS/Link-16 waveform by 2.6 dB and 2.5 dB for coherent and noncoherent detection, respectively, when $P_b = 10^{-5}$. Moreover, in an AWGN only environment, the alternative waveform with a diversity of two outperforms the JTIDS/Link-16 waveform by 3.15 dB and 2.3 dB for coherent and noncoherent detection, respectively, when $P_b = 10^{-5}$.

When PNI is also present, the proposed waveform performs better than the original JTIDS/Link-16 waveform in all the cases considered. Although the performance of the proposed waveform with a diversity of two and noncoherent detection in an AWGN plus PNI environment was analyzed, its comparison with the respective JTIDS/Link-16 double-pulse structure is left for future work.

Finally, we should note that in all cases the improvement in performance comes with a throughput increase of 33%.

Recently, soft decision decoding has been shown to be practical for RS codes. Future work should investigate the effect of soft decision decoding on the alternative waveform. In addition, future work should examine the effectiveness of realistic side information.

THIS PAGE INTENTIONALLY LEFT BLANK

LIST OF REFERENCES

- [1] General Services Administration (2009, October 11). Federal Standard 1037C. Available: [http://en.wikipedia.org/wiki/Data link](http://en.wikipedia.org/wiki/Data_link)
- [2] C. Kopp, “Network Centric Warfare Fundamentals—Part 3: JTIDS/MIDS,” *Defence TODAY Magazine*, pp. 12–19, September 2005.
- [3] D. Lekkakos, “Performance Analysis of a Link-16/JTIDS Compatible Waveform Transmitted Over a Channel with Pulse-Noise Interference,” Master’s thesis, Naval Postgraduate School, Monterey, CA, 2008.
- [4] C.-H. Kao, “Performance Analysis of a JTIDS/Link-16-Type Waveform Transmitted Over Slow, Flat Nakagami Fading Channels in the Presence of Narrowband Interference” Dissertation, Naval Postgraduate School, Monterey, CA, 2008.
- [5] I. Koromilas, “Performance Analysis of the Link-16/JTIDS Waveform With Concatenated Coding,” Master’s thesis, Naval Postgraduate School, Monterey, CA, 2009.
- [6] C. Robertson, Notes for EC4550 (Digital Communications), Naval Postgraduate School, Monterey, CA, 2005 (unpublished).
- [7] B. Sklar, *Digital Communications: Fundamentals and Applications*, 2nd ed., Upper Saddle River, NJ, Prentice Hall PTR, 2001.
- [8] C. Robertson, Notes, “Linear Block Codes” Naval Postgraduate School, Monterey, CA, 2005 (unpublished).
- [9] J. Proakis, Salehi *Digital Communications*: 5th ed., New York, NY: McGraw-Hill, 2008.
- [10] C. Robertson, Notes, “Convolutional Codes,” Naval Postgraduate School, Monterey, CA, (unpublished).
- [11] C. Robertson, Notes, “Frequency-Hopped Spread Spectrum,” Naval Postgraduate School, Monterey, CA, (unpublished).
- [12] K. W. Ho, “Performance Analysis of an Alternative Link-16/JTIDS Waveform Transmitted Over a Channel With Pulse-Noise Interference,” Master’s thesis, Naval Postgraduate School, Monterey, CA, 2008.
- [13] W. J. Wilson, “Applying Layering Principles to Legacy Systems: Link 16 as a Case Study,” *Proc. IEEE Military Commun. Conf.*, vol. 1, pp. 526–531, October 2001.

- [14] H. Wang, J. Kuang, Z. Wang, and H. Xu, "Transmission performance Evaluation of JTIDS," *Proc. IEEE Military Commun. Conf.*, vol. 4, pp. 2264–2268, 2005.
- [15] Northrop Grumman Corporation, *Understanding Link-16: A Guidebook for New User*, San Diego, CA, September 2001.

INITIAL DISTRIBUTION LIST

1. Defense Technical Information Center
Ft. Belvoir, Virginia
2. Dudley Knox Library
Naval Postgraduate School
Monterey, California
3. Chairman
Department of Electrical and Computer Engineering
Naval Postgraduate School
Monterey, California
4. Prof. Clark Robertson
Department of Electrical and Computer Engineering
Naval Postgraduate School
Monterey, California
5. Prof. Frank Kragh
Department of Electrical and Computer Engineering
Naval Postgraduate School
Monterey, California
6. Donna Miller, Research Associate
Department of Electrical and Computer Engineering
Naval Postgraduate School
Monterey, California
7. Embassy of Greece
Office of Air Attache
Washington, District of Columbia
8. MAJ Theodoros Aivaliotis
Hellenic Air Force Staff
Athens Greece